



**NIST Technical Note
NIST TN 2274**

**Partial Elastic Shape Registration of
3D Surfaces using Dynamic
Programming**

Javier Bernal
Jim Lawrence

This publication is available free of charge from:
<https://doi.org/10.6028/NIST.TN.2274>

**NIST Technical Note
NIST TN 2274**

**Partial Elastic Shape Registration of
3D Surfaces using Dynamic
Programming**

Javier Bernal

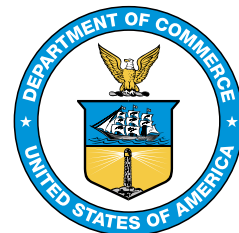
*Information Technology Laboratory
Applied and Computational Mathematics Division*

Jim Lawrence

*George Mason University
Information Technology Laboratory
Applied and Computational Mathematics Division*

This publication is available free of charge from:
<https://doi.org/10.6028/NIST.TN.2274>

November 2023



U.S. Department of Commerce
Gina M. Raimondo, Secretary

National Institute of Standards and Technology
Laurie E. Locascio, NIST Director and Under Secretary of Commerce for Standards and Technology

Certain commercial equipment, instruments, or materials, commercial or non-commercial, are identified in this paper in order to specify the experimental procedure adequately. Such identification does not imply recommendation or endorsement of any product or service by NIST, nor does it imply that the materials or equipment identified are necessarily the best available for the purpose.

NIST Technical Series Policies

[Copyright, Use, and Licensing Statements](#)

[NIST Technical Series Publication Identifier Syntax](#)

Publication History

Approved by the NIST Editorial Review Board on 2023-10-26

How to cite this NIST Technical Series Publication:

Javier Bernal, Jim Lawrence (2023) Partial Elastic Shape Registration of 3D Surfaces using Dynamic Programming. (National Institute of Standards and Technology, Gaithersburg, MD), NIST TN 2274.
<https://doi.org/10.6028/NIST.TN.2274>

NIST Author ORCID iDs

Javier Bernal: 0000-0002-9681-7007

Jim Lawrence: 0000-0003-0638-2559

Contact Information

javier.bernal@nist.gov

Abstract

The computation of the elastic shape registration of two simple surfaces in 3—dimensional space and therefore of the elastic shape distance between them has been investigated by Kurtek, Jermyn, et al. who have proposed algorithms to carry out this computation. These algorithms accomplish this by minimizing a distance function between the surfaces in terms of rotations and reparametrizations of one of the surfaces, the optimization over reparametrizations using a gradient approach that may produce a local solution. Now minimizing in terms of rotations and a special subset of the set of reparametrizations, we propose an algorithm for minimizing the distance function, the optimization over reparametrizations based on dynamic programming. This approach does not necessarily produce an optimal solution for the registration and distance problem, but perhaps a solution closer to optimal than the local solution that an algorithm with a gradient approach for optimizing over the entire set of reparametrizations may produce. In fact we propose that when computing the elastic shape registration of two simple surfaces and the elastic shape distance between them with an algorithm based on a gradient approach for optimizing over the entire set of reparametrizations, to use as the input initial solution the optimal rotation and reparametrization computed with our proposed algorithm.

Keywords

dynamic programming; elastic shape distance; homeomorphism; rotation matrix; shape analysis; singular value decomposition.

Table of Contents

1. Introduction	1
2. Homeomorphisms and the Area of a Surface	3
3. The Shape Function of a Parametrized Surface	6
4. The Elastic Shape Distance between Surfaces	9
5. Computation of Homeomorphism for Partial Registration of Surfaces using Dynamic Programming	11
6. Computation of Rotation Matrix for Rigid Alignment of Surfaces	14
7. Procedure for Optimizing over both Rotations and Reparametrizations using Dynamic Programming	16
8. Results from Implementation of Methods	18
9. Summary	29
References	30

List of Figures

Fig. 1.	Two views of the boundaries of the same two surfaces in 3-dimensional space, each of sinusoidal shape. Their shapes are essentially identical; thus the elastic shape distance between them should be essentially zero.	2
Fig. 2.	Three plots of boundaries of surfaces of the sine kind. A partial elastic shape registration of the two surfaces in each plot and the elastic shape distance between them associated with the registration were computed.	21
Fig. 3.	Graphs of optimal diffeomorphisms from execution of Dynamic Programming software on the three pairs of surfaces with $\gamma(r, t) = (r^{5/4}, t)$, $(r, t) \in [0, 1] \times [0, 1]$. One per pair, as for each pair the same two curves in 3-d space were used as input to the software each time it was executed. Thus the same diffeomorphism was computed each time for each pair of surfaces.	22
Fig. 4.	With $\gamma(r, t) = (r^{5/4}, t)$, $(r, t) \in [0, 1] \times [0, 1]$, views of boundaries of pair of surfaces in the rightmost plot in Figure 2 before computation of partial elastic shape registration (leftmost plot here), of boundary of optimally rotated first surface (middle plot), and of boundary of optimally reparametrized second surface (rightmost plot) after computations.	23
Fig. 5.	For $\gamma(r, t) = (r^{5/4}, t^{5/4})$, $(r, t) \in [0, 1] \times [0, 1]$, views of graph of optimal diffeomorphism computed the 51 st time the Dynamic Programming software was executed (leftmost plot), of boundary of optimally rotated first surface (middle plot), and of optimally reparametrized second surface (rightmost plot) after computation of partial elastic shape registration.	23
Fig. 6.	Boundaries of two surfaces of similar shape of the helicoid kind for $k = 4$, type 1 in red, type 2 in blue.	24

- Fig. 7. For $\gamma(r,t) = (r^{5/4}, t)$, $(r,t) \in [0,1] \times [0,1]$, views of graph of optimal diffeomorphism computed each time the Dynamic Programming software was executed on pair of surfaces (leftmost plot), of boundary of optimally rotated first surface (middle plot), and of optimally reparametrized second surface (rightmost plot) after computation of partial elastic shape registration. 25
- Fig. 8. For $\gamma(r,t) = (r^{5/4}, t^{5/4})$, $(r,t) \in [0,1] \times [0,1]$, views of graph of optimal diffeomorphism computed the 51st time the Dynamic Programming software was executed (leftmost plot), of boundary of optimally rotated first surface (middle plot), and of optimally reparametrized second surface (rightmost plot) after computation of partial elastic shape registration. 26
- Fig. 9. Boundaries of two surfaces of similar shape of the cosine-sine kind, type 1 in red, type 2 in blue. 27
- Fig. 10. For $\gamma(r,t) = (r^{5/4}, t)$, $(r,t) \in [0,1] \times [0,1]$, views of graph of optimal diffeomorphism computed the 51st time the Dynamic Programming software was executed on pair of surfaces (leftmost plot), of boundary of optimally rotated first surface (middle plot), and of optimally reparametrized second surface (rightmost plot) after computation of partial registration. 28
- Fig. 11. For $\gamma(r,t) = (r^{5/4}, t^{5/4})$, $(r,t) \in [0,1] \times [0,1]$, views of graph of optimal diffeomorphism computed the 51st time the Dynamic Programming software was executed (leftmost plot), of boundary of optimally rotated first surface (middle plot), and of optimally reparametrized second surface (rightmost plot) after computation of partial elastic shape registration. 28

1. Introduction

In this paper, we address the problem of computing the elastic shape registration of two simple surfaces in 3-dimensional space or equivalently the problem of computing the elastic shape distance between two such surfaces. Similar work has been carried out by Kurtek, Jermyn et al. [6, 10]. We do this first through the careful development, independently of analogous work in [6, 10], of the mathematical framework necessary for the elastic shape analysis of 3-dimensional surfaces, which culminates with the definition and justification of the distance between two such surfaces. This distance, and therefore the registration, is the result of minimizing a distance function in terms of rotations and reparametrizations of one of the surfaces. Finally, we propose an algorithm that minimizes the distance function in terms of rotations and a special subset of the set of reparametrizations, the optimization over reparametrizations based on Dynamic Programming. Obviously this approach does not necessarily produce an optimal solution for the registration and distance problem, but perhaps a solution closer to optimal than the local solution that an algorithm with a gradient approach for optimizing over the entire set of reparametrizations, such as those proposed in [6, 10], may produce. In fact we propose that when computing the elastic shape registration of two simple surfaces and the elastic shape distance between them with an algorithm based on a gradient approach for optimizing over the entire set of reparametrizations, to use as the input initial solution the optimal rotation and reparametrization computed with our proposed algorithm.

Given that S_1 and S_2 are the two surfaces under consideration, we assume they are *simple*, that is, we assume elementary regions D and E in the xy plane (\mathbb{R}^2) exist together with one-to-one functions c_1 and c_2 of class C^1 , $c_1 : D \rightarrow \mathbb{R}^3$, $c_2 : E \rightarrow \mathbb{R}^3$, such that $S_1 = c_1(D)$ and $S_2 = c_2(E)$. We then say that c_1 and c_2 *parametrize* or are *parametrizations* of S_1 and S_2 , respectively, with domains D and E , respectively, and that S_1 and S_2 are *parametrized surfaces* relative to c_1 and c_2 , respectively, with domains D and E , respectively. We note that an *elementary region* in the xy plane is one defined by restricting one of x and y to be between or equal to one of two continuous functions of the remaining variable, the remaining variable restricted to be in a bounded closed line segment. Actually, for the sake of simplicity, starting in Section 4 of this paper, we restrict ourselves to exactly one elementary region, namely $[0, 1] \times [0, 1]$, the unit square in the xy plane (\mathbb{R}^2). Accordingly, starting in Section 4, we take $D = E = [0, 1] \times [0, 1]$, and since in practice we can only work with discretizations of the surfaces S_1 , S_2 , given by c_1 , c_2 , D , E above, we assume that for positive integers M , N , not necessarily equal, and partitions of $[0, 1]$, $\{r_i\}_{i=1}^M$, $r_1 = 0 < r_2 < \dots < r_M = 1$, $\{t_j\}_{j=1}^N$, $t_1 = 0 < t_2 < \dots < t_N = 1$, not necessarily uniform, c_1 and c_2 are given as lists of $M \times N$ points in S_1 and S_2 , respectively, the lists corresponding to $c_1(r_i, t_j)$ and $c_2(r_i, t_j)$, $i = 1, \dots, M$, $j = 1, \dots, N$, respectively, and for $k = 1, 2$, given in the order $c_k(r_1, t_1)$, $c_k(r_2, t_1)$, \dots , $c_k(r_M, t_1)$, \dots , $c_k(r_1, t_N)$, $c_k(r_2, t_N)$, \dots , $c_k(r_M, t_N)$. Points $(0, 0)$, $(1, 0)$, $(1, 1)$, $(0, 1)$ are the corners of the unit square, and for $k = 1, 2$, we can think of $c_k(0, 0)$, $c_k(1, 0)$, $c_k(1, 1)$, $c_k(0, 1)$ as the ‘corners’ of the surface S_k . For the purpose

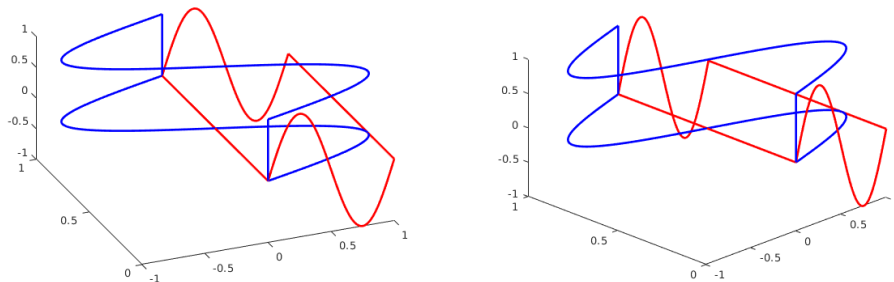


Fig. 1. Two views of the boundaries of the same two surfaces in 3-dimensional space, each of sinusoidal shape. Their shapes are essentially identical; thus the elastic shape distance between them should be essentially zero.

of comparing the shapes of the two surfaces, for each ‘corner’ of S_2 we adjust the list of points for c_2 so that the ‘corner’ is the first point in the list, and use this list together with the list for c_1 to compute a tentative elastic shape distance and registration between the surfaces. A similar computation is also carried out for the same ‘corner’ with the adjusted list for c_2 in the ‘reversed’ direction (the list for c_2 in the ‘reversed’ direction is given in the order $c_2(r_1, t_1), c_2(r_1, t_2), \dots, c_2(r_1, t_N), \dots, c_2(r_M, t_1), c_2(r_M, t_2), \dots, c_2(r_M, t_N)$). As S_2 has four ‘corners’, eight tentative elastic shape distances are then obtained and the smallest among them determines the correct elastic registration of the surfaces. Of course if enough information about the surfaces is available some of the computations of the tentative elastic shape distances can be avoided and depending on which take place, M may have to equal N , the partitions $\{r_i\}_{i=1}^M$ and $\{t_j\}_{j=1}^N$ may have to be equal, and one or both of them may have to be uniform. For simplicity, in the rest of the paper, given two simple surfaces S_1, S_2 , as above, we assume the list for c_2 suffices as it is, so that only one tentative elastic shape distance (the correct one) is computed.

Being able to compute the elastic shape registration of two surfaces in 3-dimensional space and the elastic shape distance between them could be useful in studying geological terrains, surfaces of anatomical objects such as facial surfaces, etc. See Figure 1 that depicts two such surfaces (actually their boundaries), each of sinusoidal shape. (Note that in the plots there, the x –, y – and z – axes are not to scale relative to one another).

In Section 2 of this paper, we define homeomorphisms and present some known results about them useful in the context of parametrized simple surfaces in 3–dimensional space. In particular, we prove the well-known result that the area of one such surface does not change if its parametrization is changed. In Section 3, inspired by the definition of the shape function of a parametrized curve in d –dimensional space, d any positive integer, and known results about it, we define the shape function of a parametrized simple surface in 3–dimensional space and present some fundamental results about this function. In

Section 4, given two parametrized simple surfaces of unit area in the form of their shape functions, we associate with them a double integral in terms of rotations of one of the surfaces, and C^1 homeomorphisms with Jacobians of positive determinant, each homeomorphism corresponding to a reparametrization of the same surface. We then define the elastic shape distance between the two surfaces as the result of minimizing this double integral with respect to the aforementioned rotations and homeomorphisms, and justify it accordingly. In Section 5, given two parametrized simple surfaces of unit area, again in the form of their shape functions, for a fixed rotation, we describe the computation, based on Dynamic Programming, of a homeomorphism for partially minimizing the aforementioned double integral, that is, for partially computing the elastic shape registration of the two surfaces. In Section 6, for a fixed homeomorphism, we describe the computation of a rotation matrix for approximately minimizing the integral, that is, for approximately computing the rigid alignment of the two surfaces. In Section 7, we note that the elastic shape distance between the two surfaces, still in the form of their shape functions, can also be computed in terms of another double integral that allows for one surface to be reparametrized while the other one is rotated. We then present a procedure for partially minimizing this other integral, Procedure DP-surface-min, that alternates computations of optimal homeomorphisms using Dynamic Programming as described in Section 5, and optimal rotation matrices as described in Section 6. Finally, in Section 8, we present results obtained with an implementation of our methods.

2. Homeomorphisms and the Area of a Surface

In this section we present three known results. The first two are about homeomorphisms useful in the context of parametrized surfaces in 3-dimensional space, and the third one is about the computation of the area of one such surface. We note that a *homeomorphism* is a one-to-one continuous function from a topological space onto another that has a continuous inverse function. Since simply connected domains are addressed in the first two results that follow, we also note that a *simply connected domain* is a path-connected domain where one can continuously shrink any simple closed curve into a point while remaining in the domain. For two-dimensional regions, a simply connected domain is one without holes in it. The first result that follows is a standard result in the field of topology.

Theorem 1: If X and Y are homeomorphic topological spaces, then X is simply connected if and only if Y is simply connected.

Theorem 2: Given D , a compact simply connected subset of \mathbb{R}^2 , and $h : D \rightarrow \mathbb{R}^2$, a homeomorphism, then h maps the boundary of D to exactly the boundary of $h(D)$.

Proof: Clearly $h(D)$ is closed as it is a compact subset of \mathbb{R}^2 , and by Theorem 1 it is simply connected in \mathbb{R}^2 . Let p be a point in the boundary of D . Then h restricted to $D \setminus \{p\}$ is a homeomorphism onto $h(D) \setminus h(p)$. Since $D \setminus \{p\}$ is simply connected, it must be that

$h(D) \setminus h(p)$ is simply connected as well so that $h(p)$ cannot be in the interior of $h(D)$, thus must be in its boundary. On the other hand, if q is in the boundary of $h(D)$, then through a similar argument since q is in $h(D)$ ($h(D)$ is closed), it can be shown that $h^{-1}(q)$ is in the boundary of $h^{-1}(h(D)) = D$. Thus h maps the boundary of D to exactly the boundary of $h(D)$. \square

In what follows, given a surface S in 3-dimensional space, elementary regions D , E in \mathbb{R}^2 , and one-to-one functions c , p of class C^1 , $c : D \rightarrow \mathbb{R}^3$, $p : E \rightarrow \mathbb{R}^3$, $c(D) = S$, $p(E) = S$, so that c and p are parametrizations of S with domain D and E , respectively, we say p is a *reparametrization* of c or that p *reparametrizes* S (given as an image of c), if $p = c \circ h$ for a C^1 homeomorphism h from E onto D . For (u, v) in D , writing $c(u, v) = (x(u, v), y(u, v), z(u, v))$, then given a point (u_0, v_0) in D , the vector tangent to the surface S at $c(u_0, v_0)$ in the u direction is given by

$$\frac{\partial c}{\partial u}(u_0, v_0) = \left(\frac{\partial x}{\partial u}(u_0, v_0), \frac{\partial y}{\partial u}(u_0, v_0), \frac{\partial z}{\partial u}(u_0, v_0) \right),$$

and in the v direction by

$$\frac{\partial c}{\partial v}(u_0, v_0) = \left(\frac{\partial x}{\partial v}(u_0, v_0), \frac{\partial y}{\partial v}(u_0, v_0), \frac{\partial z}{\partial v}(u_0, v_0) \right).$$

We say the surface S is *regular* (relative to the parametrization c) if at every point $c(u_0, v_0)$ in S the cross product $\frac{\partial c}{\partial u}(u_0, v_0) \times \frac{\partial c}{\partial v}(u_0, v_0)$ is nonzero. We note that if S is regular, then at every point $c(u_0, v_0)$ in S , $\frac{\partial c}{\partial u}(u_0, v_0) \times \frac{\partial c}{\partial v}(u_0, v_0)$ is a nonzero vector normal to S at $c(u_0, v_0)$.

With c , D , S , $\frac{\partial c}{\partial u}(u_0, v_0)$, $\frac{\partial c}{\partial v}(u_0, v_0)$ as above, S regular (relative to c), the surface area $A(S)$ of the parametrized surface S is given by

$$A(S) = \int \int_D \left\| \frac{\partial c}{\partial u}(u, v) \times \frac{\partial c}{\partial v}(u, v) \right\| du dv$$

where $\|\cdot\|$ is the 3-dimensional Euclidean norm.

With c , D , p , E , S , $\frac{\partial c}{\partial u}(u_0, v_0)$, $\frac{\partial c}{\partial v}(u_0, v_0)$, h as above so that p is also a parametrization of S with domain E , and p is a reparametrization of c , $p = c \circ h$, the result that follows shows the surface area $A(S)$ of S does not change if it is computed with the parametrization p of S with domain E instead of the parametrization c of S with domain D . For (r, t) in E , writing $h(r, t) = (u(r, t), v(r, t))$, and letting $\frac{\partial(u, v)}{\partial(r, t)}$ be the determinant of the Jacobian of h , $\frac{\partial(u, v)}{\partial(r, t)}$ is assumed to be nonzero on E . Finally, for (r, t) in E , writing $p(r, t) = (\hat{x}(r, t), \hat{y}(r, t), \hat{z}(r, t))$, then given a point (r_0, t_0) in E , the vector tangent to the surface S at $p(r_0, t_0)$ in the r direction is given by

$$\frac{\partial p}{\partial r}(r_0, t_0) = \left(\frac{\partial \hat{x}}{\partial r}(r_0, t_0), \frac{\partial \hat{y}}{\partial r}(r_0, t_0), \frac{\partial \hat{z}}{\partial r}(r_0, t_0) \right),$$

and in the t direction by

$$\frac{\partial p}{\partial t}(r_0, t_0) = \left(\frac{\partial \hat{x}}{\partial t}(r_0, t_0), \frac{\partial \hat{y}}{\partial t}(r_0, t_0), \frac{\partial \hat{z}}{\partial t}(r_0, t_0) \right).$$

Theorem 3: Given $c, D, p, E, S, \frac{\partial c}{\partial u}(u_0, v_0), \frac{\partial c}{\partial v}(u_0, v_0), \frac{\partial p}{\partial r}(r_0, t_0), \frac{\partial p}{\partial t}(r_0, t_0), h, \frac{\partial(u,v)}{\partial(r,t)}$ as above, then S is regular relative to p and

$$\int \int_E \left\| \frac{\partial p}{\partial r}(r, t) \times \frac{\partial p}{\partial t}(r, t) \right\| dr dt = \int \int_D \left\| \frac{\partial c}{\partial u}(u, v) \times \frac{\partial c}{\partial v}(u, v) \right\| du dv.$$

Proof: With $(u(r, t), v(r, t)) = h(r, t)$, then

$$p(r, t) = c(h(r, t)) = c(u(r, t), v(r, t)),$$

so that

$$\frac{\partial p}{\partial r} = \frac{\partial c}{\partial u} \frac{\partial u}{\partial r} + \frac{\partial c}{\partial v} \frac{\partial v}{\partial r}, \quad \frac{\partial p}{\partial t} = \frac{\partial c}{\partial u} \frac{\partial u}{\partial t} + \frac{\partial c}{\partial v} \frac{\partial v}{\partial t}.$$

Thus

$$\begin{aligned} \frac{\partial p}{\partial r} \times \frac{\partial p}{\partial t} &= \left(\frac{\partial c}{\partial u} \frac{\partial u}{\partial r} + \frac{\partial c}{\partial v} \frac{\partial v}{\partial r} \right) \times \left(\frac{\partial c}{\partial u} \frac{\partial u}{\partial t} + \frac{\partial c}{\partial v} \frac{\partial v}{\partial t} \right) \\ &= \left(\frac{\partial c}{\partial u} \times \frac{\partial c}{\partial v} \right) \left(\frac{\partial u}{\partial r} \frac{\partial v}{\partial t} \right) + \left(\frac{\partial c}{\partial v} \times \frac{\partial c}{\partial u} \right) \left(\frac{\partial v}{\partial r} \frac{\partial u}{\partial t} \right) \\ &= \left(\frac{\partial c}{\partial u} \times \frac{\partial c}{\partial v} \right) \left(\frac{\partial u}{\partial r} \frac{\partial v}{\partial t} - \frac{\partial v}{\partial r} \frac{\partial u}{\partial t} \right) \\ &= \left(\frac{\partial c}{\partial u} \times \frac{\partial c}{\partial v} \right) \frac{\partial(u, v)}{\partial(r, t)} \end{aligned}$$

so that S is regular relative to p since both $\frac{\partial c}{\partial u} \times \frac{\partial c}{\partial v}$ and $\frac{\partial(u,v)}{\partial(r,t)}$ are nonzero on E , and

$$\begin{aligned} \int \int_E \left\| \frac{\partial p}{\partial r} \times \frac{\partial p}{\partial t} \right\| dr dt &= \int \int_E \left\| \left(\frac{\partial c}{\partial u} \times \frac{\partial c}{\partial v} \right) \frac{\partial(u, v)}{\partial(r, t)} \right\| dr dt \\ &= \int \int_E \left\| \frac{\partial c}{\partial u} \times \frac{\partial c}{\partial v} \right\| \left| \frac{\partial(u, v)}{\partial(r, t)} \right| dr dt \\ &= \int \int_D \left\| \frac{\partial c}{\partial u} \times \frac{\partial c}{\partial v} \right\| du dv \end{aligned}$$

by the change of variables formula. □

3. The Shape Function of a Parametrized Surface

In this section we define the shape function of a parametrized surface in 3-dimensional space and present some fundamental results about this function. A similar definition and similar results have been presented in [2, 4, 7, 14, 15] in the context of the shape function of a parametrized curve in d -dimensional space, d any positive integer. Accordingly, in [2, 4, 7, 14, 15], given $\beta : [0, 1] \rightarrow \mathbb{R}^d$ of class C^1 , a parametrization of a curve in \mathbb{R}^d , the shape function q of β , i.e., the shape function q of the curve that β parametrizes relative to β , $q : [0, 1] \rightarrow \mathbb{R}^d$, is defined by $q(t) = \dot{\beta}(t) / \sqrt{\|\dot{\beta}(t)\|}$, $t \in [0, 1]$ (d -dimensional 0 if $\dot{\beta}(t)$ equals d -dimensional 0). It follows then that q is square integrable as

$$\int_0^1 \|q(t)\|^2 dt = \int_0^1 \|\dot{\beta}(t) / \sqrt{\|\dot{\beta}(t)\|}\|^2 dt = \int_0^1 \|\dot{\beta}(t)\| dt$$

which is the length of the curve that β parametrizes, where $\|\cdot\|$ is the d -dimensional Euclidean norm. Note that in what follows we ignore the usual definition of a diffeomorphism and refer to homeomorphisms on $[0, 1]$ as diffeomorphisms in order to distinguish them from homeomorphisms on elementary regions in the plane. Again with q the shape function of β and Γ the set of C^1 orientation-preserving diffeomorphisms of $[0, 1]$ so that for $\gamma \in \Gamma$ then $\dot{\gamma} \geq 0$ on $[0, 1]$, it then follows that for $\gamma \in \Gamma$ the shape function of the reparametrization $\beta \circ \gamma$ of β is $(q, \gamma) = (q \circ \gamma) \sqrt{\dot{\gamma}}$. With $\|q\|_2 = (\int_0^1 \|q(t)\|^2 dt)^{1/2}$, we also note that given $\beta_1, \beta_2 : [0, 1] \rightarrow \mathbb{R}^d$ of class C^1 , parametrizations of curves in \mathbb{R}^d with shape functions q_1, q_2 , respectively, then $\|(q_1, \gamma) - (q_2, \gamma)\|_2 = \|q_1 - q_2\|_2$ for any $\gamma \in \Gamma$, and from this, with $\Gamma_0 = \{\gamma \in \Gamma, \dot{\gamma} > 0 \text{ on } [0, 1]\}$, it has been demonstrated [2, 14] that ignoring rotations, the number $\inf_{\gamma \in \Gamma_0} \|q_1 - (q_2, \gamma)\|_2$ can then be used as a well-defined distance between the two curves that β_1, β_2 parametrize, β_1 and β_2 both normalized to parametrize curves of length 1.

With $c, D, S, \frac{\partial c}{\partial u}, \frac{\partial c}{\partial v}$ as in the previous section, S regular (relative to c), following the idea of the definition of the shape function of a parametrized curve in d -dimensional space as described above, we define the shape function q of the parametrization c of S with domain D , i.e., the shape function q of the surface S relative to its parametrization c with domain D , $q : D \rightarrow \mathbb{R}^3$, so that

$$\int \int_D \|q(u, v)\|^2 du dv = \int \int_D \left\| \frac{\partial c}{\partial u} \times \frac{\partial c}{\partial v} \right\| du dv$$

which is the surface area of S . This is easily seen to be indeed the case if we define the shape function q of c on D by

$$q = \left(\frac{\partial c}{\partial u} \times \frac{\partial c}{\partial v} \right) / \sqrt{\left\| \frac{\partial c}{\partial u} \times \frac{\partial c}{\partial v} \right\|}.$$

We do define q this way and note that this definition of the shape function of a surface relative to a parametrization of the surface, is slightly different from the one in [10] but similar to the one in [6]. We also note that if we allow $\frac{\partial c}{\partial u} \times \frac{\partial c}{\partial v}$ to be 3-dimensional zero at certain points, then q is defined to be 3-dimensional zero at those points.

With c, q, D, S as above, the following result, similar to the one mentioned above in the context of the shape function of the parametrization of a curve in d -dimensional space, shows how to compute the shape function of a reparametrization of c from the shape function q of c . Here p is the reparametrization of c , i.e., for an elementary region E in \mathbb{R}^2 , p is a parametrization of S with domain E , and $p = c \circ h$ for a C^1 homeomorphism h from E onto D . Assuming $\frac{\partial(u,v)}{\partial(r,t)} \geq 0$ on E , $\frac{\partial(u,v)}{\partial(r,t)}$ the determinant of the Jacobian of h , we define a function on E into \mathbb{R}^3 , which we denote by (q, h) , as follows:

$$(q, h) \equiv (q \circ h) \sqrt{\frac{\partial(u,v)}{\partial(r,t)}}.$$

Theorem 4: Given c, q, D, p, h, E, S , $\frac{\partial(u,v)}{\partial(r,t)}$ as above, the shape function on E of the reparametrization $p = c \circ h$ of c is then (q, h) .

Proof: With $(u(r,t), v(r,t)) = h(r,t)$, so that

$$p(r,t) = c(h(r,t)) = c(u(r,t), v(r,t)),$$

then on E , as established in the proof of Theorem 3, we have

$$\frac{\partial p}{\partial r} \times \frac{\partial p}{\partial t} = \left(\frac{\partial c}{\partial u} \times \frac{\partial c}{\partial v} \right) \frac{\partial(u,v)}{\partial(r,t)}.$$

Thus, if \hat{q} is the shape function of p on E , from the definition of a shape function it must then be that

$$\begin{aligned} \hat{q} &= \left(\frac{\partial p}{\partial r} \times \frac{\partial p}{\partial t} \right) / \sqrt{\left\| \frac{\partial p}{\partial r} \times \frac{\partial p}{\partial t} \right\|} \\ &= \left(\frac{\partial c}{\partial u} \times \frac{\partial c}{\partial v} \right) \frac{\partial(u,v)}{\partial(r,t)} / \sqrt{\left\| \left(\frac{\partial c}{\partial u} \times \frac{\partial c}{\partial v} \right) \frac{\partial(u,v)}{\partial(r,t)} \right\|} \\ &= \left(\left(\frac{\partial c}{\partial u} \times \frac{\partial c}{\partial v} \right) / \sqrt{\left\| \frac{\partial c}{\partial u} \times \frac{\partial c}{\partial v} \right\|} \right) \sqrt{\frac{\partial(u,v)}{\partial(r,t)}} \\ &= (q \circ h) \sqrt{\frac{\partial(u,v)}{\partial(r,t)}} = (q, h). \end{aligned}$$

□

Other results about shape functions of parametrized surfaces, similar to results about shape functions of parametrized curves in d -dimensional space [2, 14], can be developed. Given $c, q, p, h, D, E, S, \frac{\partial(u,v)}{\partial(r,t)}$ as above, q the shape function of c , $p = c \circ h$, h a C^1 homeomorphism from E onto D , $\frac{\partial(u,v)}{\partial(r,t)}$ the determinant of the Jacobian of h , assuming now $\frac{\partial(u,v)}{\partial(r,t)} > 0$ on E , so that $\frac{\partial(r,t)}{\partial(u,v)}(u,v) = (\frac{\partial(u,v)}{\partial(r,t)}(r,t))^{-1}$, $\frac{\partial(r,t)}{\partial(u,v)}$ the determinant of the Jacobian of h^{-1} on D , then with (q, h) as defined above, one such result is that $((q, h), h^{-1}) = q$ on D . This result together with the theorem that follows are of importance in the next section for justifying the definition of the distance between surfaces in a manner similar to the way the definition of the distance between curves in d -dimensional space is justified [2, 14]. The theorem shows homeomorphisms act by isometries on shape functions of parametrized surfaces.

Theorem 5: Given $D, E, h, \frac{\partial(u,v)}{\partial(r,t)}$ as above, $\frac{\partial(u,v)}{\partial(r,t)} \geq 0$ on E ; S_1, S_2 surfaces, c_1, c_2 parametrizations of S_1, S_2 , respectively, both with domain D ; p_1, p_2 parametrizations of S_1, S_2 , respectively, both with domain E ; p_1, p_2 reparametrizations of c_1, c_2 , respectively, $p_1 = c_1 \circ h, p_2 = c_2 \circ h$; $q_1, q_2, \hat{q}_1, \hat{q}_2$ the shape functions of c_1, c_2, p_1, p_2 , respectively, then

$$\begin{aligned} \|\hat{q}_1 - \hat{q}_2\|_{2,E} &\equiv \left(\int \int_E \|\hat{q}_1 - \hat{q}_2\|^2 dr dt \right)^{1/2} \\ &= \left(\int \int_D \|q_1 - q_2\|^2 du dv \right)^{1/2} \\ &\equiv \|q_1 - q_2\|_{2,D}. \end{aligned}$$

Proof: From Theorem 4, $\hat{q}_1 = (q_1, h), \hat{q}_2 = (q_2, h)$, thus

$$\begin{aligned} \|\hat{q}_1 - \hat{q}_2\|_{2,E}^2 &= \int \int_E \|\hat{q}_1 - \hat{q}_2\|^2 dr dt \\ &= \int \int_E \|(q_1, h) - (q_2, h)\|^2 dr dt \\ &= \int \int_E \|(q_1 \circ h) \sqrt{\frac{\partial(u,v)}{\partial(r,t)}} - (q_2 \circ h) \sqrt{\frac{\partial(u,v)}{\partial(r,t)}}\|^2 dr dt \\ &= \int \int_E \|(q_1 \circ h) - (q_2 \circ h)\|^2 \frac{\partial(u,v)}{\partial(r,t)} dr dt \\ &= \int \int_D \|q_1 - q_2\|^2 du dv \\ &= \|q_1 - q_2\|_{2,D}^2 \end{aligned}$$

by the change of variables formula. □

4. The Elastic Shape Distance between Surfaces

In this section we define and justify the elastic shape distance between two surfaces of unit area. This is done at first in terms of C^1 homeomorphisms with Jacobians of positive determinant (each homeomorphism defines a reparametrization of one of the surfaces), and later in terms of rotations as well. Given that S_1 and S_2 are the two surfaces, we assume they are simple and are parametrized by functions with the same domain, i.e., an elementary region D in the xy plane exists together with parametrizations c_1 and c_2 with domain D of S_1 and S_2 , respectively, $c_1 : D \rightarrow \mathbb{R}^3$, $c_2 : D \rightarrow \mathbb{R}^3$, $S_1 = c_1(D)$, $S_2 = c_2(D)$. Letting Σ_0 be the set of all C^1 homeomorphisms h , from D onto D , with $\frac{\partial(u,v)}{\partial(r,t)} > 0$ on D , $\frac{\partial(u,v)}{\partial(r,t)}$ the determinant of the Jacobian of h , given that q_1 and q_2 are, respectively, the shape functions of c_1 and c_2 , then using arguments similar to arguments for justifying the definition of the distance between curves in d -dimensional space found in [2, 14], ignoring rotations, it can be demonstrated that the number

$$\inf_{h \in \Sigma_0} \|q_1 - (q_2, h)\|_{2,D} = \inf_{h \in \Sigma_0} \left(\int \int_D \|q_1 - (q_2, h)\|^2 dr dt \right)^{1/2} =$$

$$\inf_{h \in \Sigma_0} \left(\int \int_D \|q_1 - (q_2 \circ h)\|^2 \sqrt{\frac{\partial(u,v)}{\partial(r,t)}}^2 dr dt \right)^{1/2}$$

can be used as a well-defined distance between the surfaces S_1 and S_2 , c_1 and c_2 both normalized to parametrize surfaces of area equal to 1. Note that the arguments for justifying this definition of the distance between the two surfaces are in part based on Theorem 5 in the previous section and the result described in the paragraph preceding Theorem 5.

That rotations as well act by isometries on shape functions of parametrized surfaces is justified as follows. With q_1, q_2 as above, assuming R is a 3-dimensional rotation matrix, i.e., $R \in SO(3)$, $SO(3)$ the group of 3×3 orthogonal matrices of determinant equal to 1, then because R is orthogonal, it follows easily that

$$\begin{aligned} \|Rq_1 - Rq_2\|_{2,D} &= \left(\int \int_D \|Rq_1 - Rq_2\|^2 du dv \right)^{1/2} \\ &= \left(\int \int_D \|q_1 - q_2\|^2 du dv \right)^{1/2} \\ &= \|q_1 - q_2\|_{2,D}. \end{aligned}$$

Also as established in [14] for shape functions of parametrized curves in d -dimensional space, it follows by similar arguments that given $h \in \Sigma_0$, $R \in SO(3)$, D an elementary region in the xy plane, q a shape function of a surface parametrized by a function c from D into \mathbb{R}^3 , then $(Rq, h) = R(q, h)$. That is, the actions on shape functions of homeomorphisms in Σ_0 and matrices in $SO(3)$ commute. For the sake of completeness we actually present the details of the justification of this fact in what follows. However, for this purpose, we first present a well-known formula about rotations and cross products of vectors in \mathbb{R}^3 together

with its justification, again for the sake of completeness.

Lemma: Given vectors x, y in \mathbb{R}^3 , R in $SO(3)$, then $R(x \times y) = Rx \times Ry$.

Proof: Here given a, b, c in \mathbb{R}^3 , we use the identity $a \cdot (b \times c) = \det[a \ b \ c]$, where \cdot and \det denote the inner product and determinant operations, respectively. In addition, for $j = 1, 2, 3$, we let e_j be the j^{th} unit vector in \mathbb{R}^3 , and given w in \mathbb{R}^3 , we let $(w)_j$ denote the j^{th} coordinate of w . Since $\det R = 1$ and RR^T equals the identity matrix, we then have for $j = 1, 2, 3$,

$$\begin{aligned} (R(x \times y))_j &= e_j \cdot R(x \times y) = e_j^T R(x \times y) = (R^T e_j)^T (x \times y) \\ &= R^T e_j \cdot (x \times y) = \det[R^T e_j \ x \ y] \\ &= \det R \det[R^T e_j \ x \ y] = \det R [R^T e_j \ x \ y] \\ &= \det[RR^T e_j \ Rx \ Ry] = \det[e_j \ Rx \ Ry] \\ &= e_j \cdot (Rx \times Ry) = (Rx \times Ry)_j. \end{aligned}$$

Thus $R(x \times y) = Rx \times Ry$. □

With h, R, q, c as above, in order to show $(Rq, h) = R(q, h)$, we first show that the shape function of Rc on D , say \hat{q} , is Rq . From the definition of a shape function and the lemma then

$$\begin{aligned} \hat{q} &= \left(\frac{\partial Rc}{\partial u} \times \frac{\partial Rc}{\partial v} \right) / \sqrt{\left\| \frac{\partial Rc}{\partial u} \times \frac{\partial Rc}{\partial v} \right\|} = \left(R \frac{\partial c}{\partial u} \times R \frac{\partial c}{\partial v} \right) / \sqrt{\left\| R \frac{\partial c}{\partial u} \times R \frac{\partial c}{\partial v} \right\|} \\ &= R \left(\frac{\partial c}{\partial u} \times \frac{\partial c}{\partial v} \right) / \sqrt{\left\| R \left(\frac{\partial c}{\partial u} \times \frac{\partial c}{\partial v} \right) \right\|} = R \left(\frac{\partial c}{\partial u} \times \frac{\partial c}{\partial v} \right) / \sqrt{\left\| \frac{\partial c}{\partial u} \times \frac{\partial c}{\partial v} \right\|} \\ &= Rq. \end{aligned}$$

From Theorem 4 and what we just proved, it follows that the shape function of $Rc(h)$ is then (Rq, h) . On the other hand, again by Theorem 4, the shape function of $c(h)$ is (q, h) so that again by what we just proved the shape function of $R(c(h))$ must be $R(q, h)$. Since $Rc(h)$ and $R(c(h))$ are the same function, then it must be that their shape functions are the same, i.e., $(Rq, h) = R(q, h)$.

Based in part on the observations above about rotation matrices and homeomorphisms, in a manner similar to what is done in [6, 10], given $S_1, S_2, c_1, c_2, q_1, q_2$ as above, with \inf short for infimum, it can be demonstrated that the number

$$\begin{aligned} \inf_{R \in SO(3), h \in \Sigma_0} \|q_1 - R(q_2, h)\|_{2,D} = \\ \inf_{R \in SO(3), h \in \Sigma_0} \left(\int \int_D \|q_1 - R(q_2, h)\|^2 dr dt \right)^{1/2} = \end{aligned}$$

$$\inf_{R \in SO(3), h \in \Sigma_0} \left(\int \int_D \|q_1 - R(q_2 \circ h)\| \sqrt{\frac{\partial(u,v)}{\partial(r,t)}} \|^2 dr dt \right)^{1/2}$$

can be used as a well-defined distance between the surfaces S_1 and S_2 , where again $\frac{\partial(u,v)}{\partial(r,t)}$ is the determinant of the Jacobian of h , and c_1 and c_2 are both normalized to parametrize surfaces of area equal to 1. Thus, denoting $\inf_{R \in SO(3), h \in \Sigma_0} \|q_1 - R(q_2, h)\|_{2,D}$ by $\text{dist}(S_1, S_2)$, and restricting ourselves to the simpler region $D = [0, 1] \times [0, 1]$, then by Fubini's theorem, we note,

$$\begin{aligned} \text{dist}(S_1, S_2) &= \inf_{R \in SO(3), h \in \Sigma_0} \left(\int \int_D \|q_1 - R(q_2, h)\|^2 dr dt \right)^{1/2} \\ &= \inf_{R \in SO(3), h \in \Sigma_0} \left(\int_0^1 \int_0^1 \|q_1 - R(q_2, h)\|^2 dr dt \right)^{1/2} \end{aligned}$$

which we use in the next section.

5. Computation of Homeomorphism for Partial Registration of Surfaces using Dynamic Programming

In this section, ignoring rotations, we describe the computation, based on Dynamic Programming, of a homeomorphism for the partial elastic shape registration of two simple surfaces of unit area in 3-dimensional space. Given that S_1 and S_2 are the two surfaces, with $D = [0, 1] \times [0, 1]$, we assume accordingly that one-to-one functions c_1 and c_2 exist of class C^1 , $c_1 : D \rightarrow \mathbb{R}^3$, $c_2 : D \rightarrow \mathbb{R}^3$, such that $S_1 = c_1(D)$ and $S_2 = c_2(D)$. That is, c_1 and c_2 parametrize or are parametrizations of S_1 and S_2 , respectively. Given that q_1 and q_2 are, respectively, the shape functions of c_1 and c_2 , then we hope to minimize

$$\begin{aligned} \int \int_D \|q_1 - (q_2, h)\|^2 dr dt &= \int \int_D \|q_1 - (q_2 \circ h)\| \sqrt{\frac{\partial(u,v)}{\partial(r,t)}} \|^2 dr dt \\ &= \int_0^1 \int_0^1 \|q_1 - (q_2 \circ h)\| \sqrt{\frac{\partial(u,v)}{\partial(r,t)}} \|^2 dr dt \end{aligned}$$

with respect to h in Σ_0 , where Σ_0 is the set of all C^1 homeomorphisms h from D onto itself, with $\frac{\partial(u,v)}{\partial(r,t)} > 0$ on D , $\frac{\partial(u,v)}{\partial(r,t)}$ the determinant of the Jacobian of h . We note, this minimization is usually carried out with an algorithm that uses a gradient approach for the optimization over reparametrizations, i.e., over homeomorphisms h in Σ_0 , that may produce a local solution [6, 10]. In this paper we have opted to carry out the minimization with respect to h in a special subset of Σ_0 that allows for the use of Dynamic Programming. We denote this subset of Σ_0 by Σ_1 , h in Σ_1 satisfying that $h \in \Sigma_0$ and for (r, t) in D , if $h(r, t) = (\hat{r}, \hat{t})$ then it must be that $\hat{t} = t$. In addition, if $h \in \Sigma_1$, we assume for any t in $[0, 1]$ that $h(0, t) = (0, t)$ and $h(1, t) = (1, t)$. That a minimization over Σ_1 allows for the use of Dynamic Programming will become evident below. Note, from Theorem 2, with ∂D the

boundary of D , for any homeomorphism h from D onto itself, not necessarily in Σ_0 or Σ_1 , it must be that $h(\partial D) = \partial D$.

Since in practice we can only work with a discretized version of the problem, for our purposes we assume the situation is as follows: for positive integers M, N , not necessarily equal, and partitions of $[0, 1]$, $\{r_i\}_{i=1}^M$, $r_1 = 0 < r_2 < \dots < r_M = 1$, $\{t_j\}_{j=1}^N$, $t_1 = 0 < t_2 < \dots < t_N = 1$, not necessarily uniform, c_1 and c_2 are given as lists of $M \times N$ points in the surfaces S_1 and S_2 , respectively, the lists for c_1 and c_2 corresponding to $c_1(r_i, t_j)$ and $c_2(r_i, t_j)$, $i = 1, \dots, M$, $j = 1, \dots, N$, respectively; for $k = 1, 2$, the list for c_k given in the following order: $c_k(r_1, t_1), c_k(r_2, t_1), \dots, c_k(r_M, t_1), \dots, c_k(r_1, t_N), c_k(r_2, t_N), \dots, c_k(r_M, t_N)$.

Computing $\frac{\partial c_1}{\partial r}(r_i, t_j)$, $\frac{\partial c_1}{\partial t}(r_i, t_j)$, $\frac{\partial c_2}{\partial r}(r_i, t_j)$, $\frac{\partial c_2}{\partial t}(r_i, t_j)$ with centered finite differences from $c_1(r_i, t_j)$ and $c_2(r_i, t_j)$, for $i = 1, \dots, M$, $j = 1, \dots, N$, we can then approximately compute for $i = 1, \dots, M$, $j = 1, \dots, N$, $k = 1, 2$,

$$q_k(r_i, t_j) = \left(\left(\frac{\partial c_k}{\partial r} \times \frac{\partial c_k}{\partial t} \right) / \sqrt{\left\| \frac{\partial c_k}{\partial r} \times \frac{\partial c_k}{\partial t} \right\|} \right)(r_i, t_j),$$

(3-dimensional zero if $(\frac{\partial c_k}{\partial r} \times \frac{\partial c_k}{\partial t})(r_i, t_j)$ equals 3-dimensional zero).

Finally we note that if $h \in \Sigma_1$, then $h(r, t) = (u(r, t), v(r, t)) = (u(r, t), t)$ for (r, t) in D , so that $\frac{\partial v}{\partial r}(r, t) = 0$ and $\frac{\partial v}{\partial t}(r, t) = 1$, and therefore $\frac{\partial(u, v)}{\partial(r, t)}(r, t) = \frac{\partial u}{\partial r}(r, t)$ for (r, t) in D .

Given h in Σ_1 and an integer j , $1 \leq j \leq N$, next we discretize the integral

$$\int_0^1 \|q_1(r, t_j) - ((q_2 \circ h) \sqrt{\frac{\partial(u, v)}{\partial(r, t)}})(r, t_j)\|^2 dr.$$

For this purpose, we define $q_{1j}(r_i)$, $q_{2j}(r_i)$ in \mathbb{R}^3 for $i = 1, \dots, M$, by

$$q_{1j}(r_i) = q_1(r_i, t_j), \quad q_{2j}(r_i) = q_2(r_i, t_j),$$

and define as well a diffeomorphism h_j from $[0, 1]$ onto $[0, 1]$ by

$$h_j(r) = u(r, t_j), \quad r \in [0, 1].$$

Note, h_j is indeed a diffeomorphism as clearly $h_j(0) = 0$, $h_j(1) = 1$, and for $r \in [0, 1]$, $h'_j(r) = \frac{dh_j}{dr}(r) = \frac{\partial u}{\partial r}(r, t_j) = \frac{\partial(u, v)}{\partial(r, t)}(r, t_j) > 0$.

For $i = 1, \dots, M$, we can then compute $h_j(r_i) = u(r_i, t_j)$ so that $h_j(r_1) = h_j(0) = 0$ and $h_j(r_M) = h_j(1) = 1$. In addition, for $i = 1, \dots, M-1$, we compute $\Delta r_i = r_{i+1} - r_i$, approximately compute $h'_j(r_i) = (h_j(r_{i+1}) - h_j(r_i)) / \Delta r_i$, set $h'_j(r_M) = h'_j(r_1)$, and by interpolating $q_{2j}(r_i)$, $i = 1, \dots, M$, by a cubic spline, for $i = 1, \dots, M$, we can approximately compute $q_{2j}(h_j(r_i))$, which in turn is an approximation of $(q_2 \circ h)(r_i, t_j)$ as $(q_2 \circ h)(r_i, t_j) =$

$q_2(h(r_i, t_j)) = q_2(u(r_i, t_j), t_j) = q_2(h_j(r_i), t_j) = q_{2j}(h_j(r_i))$ if $q_{2j}(r)$ is interpreted to be $q_2(r, t_j)$ for every $r \in [0, 1]$. Thus, with the trapezoidal rule the integral is discretized by

$$E(h_j) = \frac{1}{2} \sum_{i=1}^{M-1} \Delta r_i (E_{i+1}^j + E_i^j)$$

where for $i = 1, \dots, M$,

$$E_i^j = \|q_{1j}(r_i) - q_{2j}(h_j(r_i))\sqrt{h'_j(r_i)}\|^2.$$

From this, again using the trapezoidal rule, we can then discretize the double integral

$$\int_0^1 \int_0^1 \|q_1(r, t) - ((q_2 \circ h) \sqrt{\frac{\partial(u, v)}{\partial(r, t)}})(r, t)\|^2 dr dt$$

by

$$E = \frac{1}{2} \sum_{j=1}^{N-1} \Delta t_j (E(h_{j+1}) + E(h_j)),$$

where for $j = 1, \dots, N-1$, $\Delta t_j = t_{j+1} - t_j$.

Given j , $1 \leq j \leq N$, treating now $h_j(r_i)$, $i = 1, \dots, M$, in the definition of $E(h_j)$ as the discretization of any diffeomorphism h_j from $[0, 1]$ onto $[0, 1]$, if for each j , $j = 1, \dots, N$, we can find h_j whose discretization minimizes $E(h_j)$, then the collection of diffeomorphisms h_j , $j = 1, \dots, N$, minimizes E , and a homeomorphism h in Σ_1 can be identified such that $h(r_i, t_j) = (h_j(r_i), t_j)$, $i = 1, \dots, M$, $j = 1, \dots, N$. Thus, the double integral above is approximately minimized by h among all homeomorphisms in Σ_1 , with the value of the double integral approximately equal to E .

In [4], algorithm *adapt-DP*, an algorithm based on Dynamic Programming, was presented for approximately computing, ignoring rotations, the elastic shape registration of two curves in d -dimensional space. The algorithm was originally presented in [1] for $d = 2$. Given that \hat{q}_1 and \hat{q}_2 are discretizations of the shape functions of the two curves, \hat{q}_1 and \hat{q}_2 are used as input for algorithm *adapt-DP* to compute a discretization of a diffeomorphism for reparametrizing the second curve, the reparametrization then resulting in an approximate elastic shape registration of the two curves. Even though for $j = 1, \dots, N$, q_{1j} and q_{2j} as defined above are not exactly computed as discretizations of the shape functions of curves in 3-dimensional space, with algorithm *adapt-DP* for $d = 3$ with q_{1j} , q_{2j} taking the place of \hat{q}_1 , \hat{q}_2 , respectively, we can still compute the discretization of some diffeomorphism h_j , i.e., $h_j(r_i)$, $i = 1, \dots, M$, that approximately minimizes $E(h_j)$. Having done this for each j , $j = 1, \dots, N$, h in Σ_1 can then be identified such that $h(r_i, t_j) = (h_j(r_i), t_j)$, $i = 1, \dots, M$, $j = 1, \dots, N$, and, ignoring rotations, c_1 , $c_2(h)$ are interpreted to achieve

approximately the partial elastic shape registration of the two surfaces. Computing $E = \frac{1}{2} \sum_{j=1}^{N-1} \Delta t_j (E(h_{j+1}) + E(h_j))$, again ignoring rotations, then \sqrt{E} is interpreted to be approximately the elastic shape distance between the two surfaces corresponding to the partial elastic shape registration of the two surfaces.

6. Computation of Rotation Matrix for Rigid Alignment of Surfaces

In this section, we describe the computation of an approximately optimal rotation matrix for the rigid alignment of two simple surfaces of unit area in 3-dimensional space. Given that S_1 and S_2 are the two surfaces, with D, c_1, c_2, q_1, q_2 as in the previous section, we hope to minimize

$$\int \int_D \|q_1(r, t) - Rq_2(r, t)\|^2 dr dt = \int_0^1 \int_0^1 \|q_1(r, t) - Rq_2(r, t)\|^2 dr dt$$

with respect to rotation matrices R in 3-dimensional space, i.e., with respect to 3×3 matrices R that are orthogonal and have determinant equal to 1, i.e., with respect to matrices R in $SO(3)$.

As in the previous section, we must work with a discretized version of the problem. Thus we assume again that for positive integers M, N , not necessarily equal, and partitions of $[0, 1]$, $\{r_i\}_{i=1}^M, r_1 = 0 < r_2 < \dots < r_M = 1, \{t_j\}_{j=1}^N, t_1 = 0 < t_2 < \dots < t_N = 1$, not necessarily uniform, c_1 and c_2 are given as lists of $M \times N$ points in the surfaces S_1 and S_2 , respectively, the lists for c_1 and c_2 corresponding to $c_1(r_i, t_j)$ and $c_2(r_i, t_j)$, $i = 1, \dots, M, j = 1, \dots, N$, respectively, and that $q_1(r_i, t_j)$ and $q_2(r_i, t_j)$ are approximately computed from $c_1(r_i, t_j)$ and $c_2(r_i, t_j)$, $i = 1, \dots, M, j = 1, \dots, N$, as in the previous section. With $\Delta r_i = r_{i+1} - r_i$, $i = 1, \dots, M-1$, for R in $SO(3)$, and an integer j , $1 \leq j \leq N$, next with the trapezoidal rule we discretize the integral

$$\int_0^1 \|q_1(r, t_j) - Rq_2(r, t_j)\|^2 dr$$

by

$$\begin{aligned} F_j &= \frac{1}{2} \sum_{i=1}^{M-1} \Delta r_i (\|q_1(r_i, t_j) - Rq_2(r_i, t_j)\|^2 + \|q_1(r_{i+1}, t_j) - Rq_2(r_{i+1}, t_j)\|^2) \\ &= \sum_{i=1}^M \Delta \tilde{r}_i \|q_1(r_i, t_j) - Rq_2(r_i, t_j)\|^2, \end{aligned}$$

where $\Delta \tilde{r}_1 = (r_2 - r_1)/2$, $\Delta \tilde{r}_M = (r_M - r_{M-1})/2$, and for $i = 2, \dots, M-1$, $\Delta \tilde{r}_i = (r_{i+1} - r_{i-1})/2$. Note, $\Delta \tilde{r}_i > 0$ for $i = 1, \dots, M$, and $\sum_{i=1}^M \Delta \tilde{r}_i = 1$.

From this, with $\Delta t_j = t_{j+1} - t_j$, $j = 1, \dots, N-1$, again using the trapezoidal rule and noting

that $\|Rq_2(r_i, t_j)\| = \|q_2(r_i, t_j)\|$, $i = 1, \dots, M$, $j = 1, \dots, N$, we can then discretize the double integral

$$\int_0^1 \int_0^1 \|q_1(r, t) - Rq_2(r, t)\|^2 dr dt$$

by

$$\begin{aligned} F &= \frac{1}{2} \sum_{j=1}^{N-1} \Delta t_j (F_{j+1} + F_j) = \sum_{j=1}^N \Delta \tilde{t}_j F_j \\ &= \sum_{j=1}^N \Delta \tilde{t}_j \left(\sum_{i=1}^M \Delta \tilde{r}_i \|q_1(r_i, t_j) - Rq_2(r_i, t_j)\|^2 \right) \\ &= \sum_{j=1}^N \Delta \tilde{t}_j \left(\sum_{i=1}^M \Delta \tilde{r}_i (\|q_1(r_i, t_j)\|^2 + \|q_2(r_i, t_j)\|^2) \right. \\ &\quad \left. - 2 \sum_{i=1}^M \Delta \tilde{r}_i ((q_1(r_i, t_j))^T R q_2(r_i, t_j)) \right), \end{aligned}$$

where $\Delta \tilde{t}_1 = (t_2 - t_1)/2$, $\Delta \tilde{t}_N = (t_N - t_{N-1})/2$, and for $j = 2, \dots, N-1$, $\Delta \tilde{t}_j = (t_{j+1} - t_{j-1})/2$. Note, $\Delta \tilde{t}_j > 0$ for $j = 1, \dots, N$, and $\sum_{j=1}^N \Delta \tilde{t}_j = 1$.

Thus, minimizing F over all rotations R in $SO(3)$ is equivalent to maximizing over the same set of rotations

$$\sum_{j=1}^N \Delta \tilde{t}_j \left(\sum_{i=1}^M \Delta \tilde{r}_i ((q_1(r_i, t_j))^T R q_2(r_i, t_j)) \right) = \text{tr}(RA^T),$$

where A is the 3×3 matrix with entries

$$A_{kl} = \sum_{j=1}^N \Delta \tilde{t}_j \left(\sum_{i=1}^M \Delta \tilde{r}_i (q_1(r_i, t_j)_k q_2(r_i, t_j)_l) \right),$$

for each pair $k, l = 1, 2, 3$, $q_1(r_i, t_j)_k$ the k^{th} coordinate of $q_1(r_i, t_j)$, and $q_2(r_i, t_j)_l$ the l^{th} coordinate of $q_2(r_i, t_j)$, $i = 1, \dots, M$, $j = 1, \dots, N$, and $\text{tr}(RA^T)$ is the trace of the matrix RA^T .

Accordingly, an optimal rotation matrix R for maximizing $\text{tr}(RA^T)$ can be computed from the singular value decomposition of A or, more precisely, with the Kabsch-Umeyama algorithm [3, 8, 9, 11, 16] (see Algorithm Kabsch-Umeyama below for 3-dimensional surfaces, where $\text{diag}\{s_1, s_2, s_3\}$ is the 3×3 diagonal matrix with numbers s_1, s_2, s_3 as the elements of the diagonal, in that order running from the upper left to the lower right of the matrix). A *singular value decomposition* (SVD) [12] of A is a representation of the form $A = USV^T$, where U and V are 3×3 orthogonal matrices and S is a 3×3 diagonal matrix with the singular values of A , which are nonnegative real numbers, appearing in the diagonal of S in descending order, from the upper left to the lower right

of S . Finally, note that the SVD concept can be generalized so that any matrix of any dimension, not necessarily square, has a singular value decomposition, not necessarily unique [12].

Algorithm Kabsch-Umeyama for surfaces (KU3 algorithm)

Set $\Delta\tilde{r}_1 = (r_2 - r_1)/2$, $\Delta\tilde{r}_M = (r_M - r_{M-1})/2$, and for $i = 2, \dots, M-1$, $\Delta\tilde{r}_i = (r_{i+1} - r_{i-1})/2$.

Set $\Delta\tilde{t}_1 = (t_2 - t_1)/2$, $\Delta\tilde{t}_N = (t_N - t_{N-1})/2$, and for $j = 2, \dots, N-1$, $\Delta\tilde{t}_j = (t_{j+1} - t_{j-1})/2$.

Set $q_1(r_i, t_j)_k$ equal to the k^{th} coordinate of $q_1(r_i, t_j)$ for $i = 1, \dots, M$, $j = 1, \dots, N$, $k = 1, 2, 3$.

Set $q_2(r_i, t_j)_l$ equal to the l^{th} coordinate of $q_2(r_i, t_j)$ for $i = 1, \dots, M$, $j = 1, \dots, N$, $l = 1, 2, 3$.

Compute $A_{kl} = \sum_{j=1}^N \Delta\tilde{t}_j (\sum_{i=1}^M \Delta\tilde{r}_i (q_1(r_i, t_j)_k q_2(r_i, t_j)_l))$
for each pair $k, l = 1, 2, 3$.

Identify 3×3 matrix A with entries A_{kl} for each pair $k, l = 1, 2, 3$.

Compute SVD of A , i.e., identify 3×3 matrices U, S, V , so that $A = USV^T$ in the SVD sense.

Set $s_1 = s_2 = 1$.

if $\det(UV) > 0$ **then** set $s_3 = 1$.

else set $s_3 = -1$. **end if**

Set $\tilde{S} = \text{diag}\{s_1, s_2, s_3\}$.

Compute and return $R = U\tilde{S}V^T$ and $\text{maxtrace} = \text{tr}(RA^T)$.

7. Procedure for Optimizing over both Rotations and Reparametrizations using Dynamic Programming

With $D = [0, 1] \times [0, 1]$, $c_1, c_2, q_1, q_2, S_1, S_2$ as above, R in $SO(3)$, h in Σ_0 , so that $\frac{\partial(u,v)}{\partial(r,t)}$, the determinant of the Jacobian of h , is positive on D , we hope to minimize

$$\int_0^1 \int_0^1 \|q_1(r, t) - (R(q_2 \circ h) \sqrt{\frac{\partial(u,v)}{\partial(r,t)}})(r, t)\|^2 dr dt$$

with respect to R and h .

We note, using arguments as those in [5], the above minimization problem can be reformulated as that of minimizing

$$\int_0^1 \int_0^1 \|Rq_1(r, t) - ((q_2 \circ h) \sqrt{\frac{\partial(u,v)}{\partial(r,t)}})(r, t)\|^2 dr dt$$

with respect to R and h .

This allows for the second surface to be reparametrized while the first one is rotated. Of course, as already noted above, we work with Σ_1 , as defined above, instead of Σ_0 of which it is a subset, as this allows for the use of Dynamic Programming when optimizing over reparametrizations of the second surface. Assuming $M, N, r_i, i = 1, \dots, M, t_j, j = 1, \dots, N, c_1(r_i, t_j), c_2(r_i, t_j), q_1(r_i, t_j), q_2(r_i, t_j), i = 1, \dots, M, j = 1, \dots, N$, are as in the previous sections, for the purpose of approximately minimizing the second double integral above with respect to R in $SO(3)$, h in Σ_1 , we use the procedure below that alternates computations of discretizations of approximately optimal homeomorphisms in Σ_1 using Dynamic Programming (one per iteration for reparametrizing the second surface) and approximately optimal rotation matrices (one per iteration for rotating the first surface), these computations as described in the previous two sections. The procedure, Procedure DP-surface-min, with $c_1(r_i, t_j), c_2(r_i, t_j), q_1(r_i, t_j), q_2(r_i, t_j), i = 1, \dots, M, j = 1, \dots, N$, as input, is summarized below. In it, given discretizations $q(r_i), \hat{q}(r_i), i = 1, \dots, M$, of functions q, \hat{q} , treated as discretizations of shape functions of curves in 3-dimensional space, to say “Execute DP algorithm for $q(r_i), \hat{q}(r_i), i = 1, \dots, M$ ” will mean the DP algorithm (*adapt-DP* for $d = 3$) should be executed with $q(r_i), \hat{q}(r_i), i = 1, \dots, M$, as input, as described in Section 5 above. Also, given $\tilde{q}_1(r_i, t_j), \tilde{q}_2(r_i, t_j), i = 1, \dots, M, j = 1, \dots, N$, discretizations of shape functions \tilde{q}_1, \tilde{q}_2 of the two surfaces, to say “Execute KU3 algorithm for $\tilde{q}_1(r_i, t_j), \tilde{q}_2(r_i, t_j), i = 1, \dots, M, j = 1, \dots, N$ ” will mean the Kabsch-Umeyama algorithm for surfaces, outlined in the previous section, should be executed with \tilde{q}_1, \tilde{q}_2 taking the place of q_1, q_2 , respectively, in the algorithm.

Procedure DP-surface-min

Set $\Delta r_i = r_{i+1} - r_i, i = 1, \dots, M - 1$.

Set $\Delta \tilde{r}_1 = (r_2 - r_1)/2, \Delta \tilde{r}_M = (r_M - r_{M-1})/2$, and for $i = 2, \dots, M - 1, \Delta \tilde{r}_i = (r_{i+1} - r_{i-1})/2$.

Set $\Delta \tilde{t}_1 = (t_2 - t_1)/2, \Delta \tilde{t}_N = (t_N - t_{N-1})/2$, and for $j = 2, \dots, N - 1, \Delta \tilde{t}_j = (t_{j+1} - t_{j-1})/2$.

Set $\hat{q}_2(r_i, t_j) = q_2(r_i, t_j)$ for $i = 1, \dots, M, j = 1, \dots, N$.

Set $iter = 0, E^{curr} = 10^6, iten = 10, tol = 10^{-6}$.

repeat

Set $iter = iter + 1, E^{prev} = E^{curr}$.

Execute KU3 algorithm for $\hat{q}_2(r_i, t_j), q_1(r_i, t_j), i = 1, \dots, M, j = 1, \dots, N$, to get rotation matrix R .

Set $\hat{q}_1(r_i, t_j) = Rq_1(r_i, t_j)$ for $i = 1, \dots, M, j = 1, \dots, N$.

for $j = 1, \dots, N$ **do**

Set $q_{1j}(r_i) = \hat{q}_1(r_i, t_j), q_{2j}(r_i) = q_2(r_i, t_j), i = 1, \dots, M$.

Execute DP algorithm for $q_{1j}(r_i), q_{2j}(r_i), i = 1, \dots, M$, to get discretization of diffeomorphism $h_j: h_j(r_i), i = 1, \dots, M$.

Set $h'_j(r_i) = (h_j(r_{i+1}) - h_j(r_i))/\Delta r_i$ for $i = 1, \dots, M - 1$,

```

 $h'_j(r_M) = h'_j(r_1).$ 
From interpolation of  $q_{2j}(r_i)$ ,  $i = 1, \dots, M$ , with a cubic spline
set  $\hat{q}_{2j}(r_i) = \sqrt{h'_j(r_i)q_{2j}(h_j(r_i))}$  for  $i = 1, \dots, M$ .
Compute  $E(h_j) = \sum_{i=1}^M \Delta \tilde{r}_i \|q_{1j}(r_i) - \sqrt{h'_j(r_i)q_{2j}(h_j(r_i))}\|^2$ 
 $= \sum_{i=1}^M \Delta \tilde{r}_i \|q_{1j}(r_i) - \hat{q}_{2j}(r_i)\|^2$ .
Set  $\hat{q}_2(r_i, t_j) = \hat{q}_{2j}(r_i)$  for  $i = 1, \dots, M$ .
end for
 $E^{curr} = \sum_{j=1}^N \Delta \tilde{t}_j E(h_j).$ 
until  $|E^{curr} - E^{prev}| < tol$  or  $iter > iten$ .
 $E = E^{curr}$ .
for  $j = 1, \dots, N$  do
Set  $h(r_i, t_j) = (h_j(r_i), t_j)$  for  $i = 1, \dots, M$ .
Set  $c_{2j}(r_i) = c_2(r_i, t_j)$  for  $i = 1, \dots, M$ .
From interpolation of  $c_{2j}(r_i)$ ,  $i = 1, \dots, M$ , with a cubic spline
set  $\hat{c}_2(r_i, t_j) = c_{2j}(h_j(r_i))$  for  $i = 1, \dots, M$ .
end for
Set  $\hat{c}_1(r_i, t_j) = Rc_1(r_i, t_j)$  for  $i = 1, \dots, M$ ,  $j = 1, \dots, N$ .
Return  $E, R, h(r_i, t_j), \hat{c}_1(r_i, t_j), \hat{q}_1(r_i, t_j), \hat{c}_2(r_i, t_j), \hat{q}_2(r_i, t_j),$ 
 $i = 1, \dots, M, j = 1, \dots, N$ .

```

On output, restricting ourselves to homeomorphisms in Σ_1 , E is interpreted to be the square of the elastic shape distance between c_1 and c_2 ; $\hat{c}_1(r_i, t_j)$ and $\hat{c}_2(r_i, t_j)$, $i = 1, \dots, M$, $j = 1, \dots, N$, are interpreted to achieve the elastic shape registration of c_1 and c_2 ; \hat{q}_1 and \hat{q}_2 are the shape functions of \hat{c}_1 and \hat{c}_2 , respectively; R is the optimal rotation matrix and h is the optimal homeomorphism in Σ_1 with which everything is computed. Everything including R and h approximately computed.

8. Results from Implementation of Methods

A software package that incorporates the methods presented in this paper for computing, using Dynamic Programming, a partial elastic shape registration of two simple surfaces in 3-dimensional space, and therefore the elastic shape distance between them associated with this partial registration, has been implemented. The implementation is in Matlab¹ with the exception of the Dynamic Programming routine which is written in Fortran but is executed as a Matlab mex file. In this section, we present results obtained from executions of the software package. We note, the software package as well as input data files, a README file, etc. can be obtained at the following link

<https://doi.org/10.18434/mds2-3056>

¹The identification of any commercial product or trade name does not imply endorsement or recommendation by the National Institute of Standards and Technology.

We note, Matlab file `ESD_driv_surf_3d.m` is the driver routine of the package, and Fortran routine `DP_MEX_WNDSTRP_ALLDIM.F` is the Dynamic Programming routine which has already been processed (with parameter `dimx = 3`) to be executed as a Matlab mex file. In case the Fortran routine must be processed to obtain a new mex file, this can be done by typing in the Matlab window:

```
mex -compatibleArrayDims DP_MEX_WNDSTRP_ALLDIM.F
```

At the start of the execution of the software, we assume S_1, S_2 are the two simple surfaces in 3-dimensional space under consideration, with functions $c_1, c_2 : D \equiv [0, T_1] \times [0, T_2] \rightarrow \mathbb{R}^3$, $T_1, T_2 > 0$, as their parametrizations, respectively, so that $S_1 = c_1(D)$, $S_2 = c_2(D)$. We also assume that as input to the software, for positive integers M, N , not necessarily equal, and partitions of $[0, T_1]$, $[0, T_2]$, respectively, $\{r_i\}_{i=1}^M$, $r_1 = 0 < r_2 < \dots < r_M = T_1$, $\{t_j\}_{j=1}^N$, $t_1 = 0 < t_2 < \dots < t_N = T_2$, not necessarily uniform, discretizations of c_1, c_2 are given, each discretization in the form of a list of $M \times N$ points in the corresponding surface, namely $c_1(r_i, t_j)$ and $c_2(r_i, t_j)$, $i = 1, \dots, M$, $j = 1, \dots, N$, respectively, and for $k = 1, 2$, as specified in the Introduction section, in the order $c_k(r_1, t_1), c_k(r_2, t_1), \dots, c_k(r_M, t_1), \dots, c_k(r_1, t_N), c_k(r_2, t_N), \dots, c_k(r_M, t_N)$. Based on this input, for the purpose of computing, using Dynamic Programming, a partial elastic shape registration of S_1 and S_2 , together with the elastic shape distance between them associated with the partial registration, the program always proceeds first to scale the partitions $\{r_i\}_{i=1}^M, \{t_j\}_{j=1}^N$, so that they become partitions of $[0, 1]$, and to compute an approximation of the area of each surface. During the execution of the software package, the former is accomplished by Matlab routine `ESD_driv_surf_3d.m`, while the latter by Matlab routine `ESD_comp_surf_3d.m` through the computation for each k , $k = 1, 2$ of the sum of the areas of triangles with vertices $c_k(r_i, t_j)$, $c_k(r_{i+1}, t_{j+1})$, $c_k(r_i, t_{j+1})$, and $c_k(r_i, t_j)$, $c_k(r_{i+1}, t_j)$, $c_k(r_{i+1}, t_{j+1})$, for $i = 1, \dots, M-1$, $j = 1, \dots, N-1$. The program then proceeds to scale the discretizations of the parametrizations of the two surfaces so that each surface has approximate area equal to 1 (given a surface and its approximate area, each point in the discretization of the parametrization of the surface is divided by the square root of half the approximate area of the surface). Once routine `ESD_comp_surf_3d.m` is done, the actual computations of the partial registration and associated elastic shape distance are carried out by Matlab routine `ESD_core_surf_3d.m` in which the methods for this purpose presented in this paper, mainly Procedure DP-surface-min in Section 7, have been implemented.

The results that follow were obtained from applications of our software package on discretizations of three kinds of surfaces in 3-dimensional space that we call surfaces of the sine, helicoid and cosine-sine kind. On input all surfaces were given as discretizations on the unit square $([0, 1] \times [0, 1])$, each interval $[0, 1]$ uniformly partitioned into 100 intervals so that the unit square was thus partitioned into 10000 squares, each square of size 0.01×0.01 , their corners making up a set of 10201 points. Using the notation used at the beginning of this section, the uniform partitions of the two $[0, 1]$ intervals that define the unit square were then $\{r_i\}_{i=1}^M, \{t_j\}_{j=1}^N$, with $M = N = 101$, $r_{101} = t_{101} = 1.0$, thus already scaled from the

start as required, and by evaluating the surfaces at the 10201 points identified above in the order as specified above and in the Introduction section, a discretization of each surface was obtained consisting of 10201 points. Given a pair of surfaces of one of the three kinds mentioned above, and given that a partial elastic shape registration of the two surfaces and the elastic shape distance between them associated with the partial registration were to be computed, one surface was identified as the first surface, the other one as the second surface (in the procedure for optimizing over rotations and reparametrizations using Dynamic Programming as described in Section 7, Procedure DP-surface-min, the second surface is reparametrized while the first one is rotated). For the purpose of testing the capability of the software for optimizing over reparametrizations based on Dynamic Programming, again using the notation used at the beginning of this section, for γ , a bijective function on the unit square to be defined below, with $(\hat{r}_i, \hat{t}_j) = \gamma(r_i, t_j)$, $i = 1, \dots, 101$, $j = 1, \dots, 101$, the second surface was reparametrized through its discretization, namely by setting $\hat{c}_2 = c_2$ and computing $c_2(r_i, t_j) = \hat{c}_2(\hat{r}_i, \hat{t}_j)$, $i = 1, \dots, 101$, $j = 1, \dots, 101$, while the first surface was kept as originally defined and discretized by computing $c_1(r_i, t_j)$, $i = 1, \dots, 101$, $j = 1, \dots, 101$. Given the pair of surfaces, the program then, using the discretizations of the surfaces as just described in terms of c_1 , c_2 , etc., after computing an approximation of the area of each surface and scaling each surface to have approximate area equal to 1, proceeded to compute a partial elastic shape registration of the two surfaces and the elastic shape distance between them associated with the partial registration. We note that because N equaled 101, during the execution the software package, the Dynamic Programming software was executed 101 times each time the **repeat** loop in Procedure DP-surface-min was executed. Finally, we note again that in what follows we refer to homeomorphisms on $[0, 1]$ as diffeomorphisms in order to distinguish them from homeomorphisms on the unit square in the plane.

The first results that follow were obtained from applications of our software package on discretizations of surfaces in 3-dimensional space that are actually graphs of 3-dimensional functions based on the sine curve. Given k , a positive integer, one type of surface to which we refer as a surface of the sine kind (type 1) is defined by

$$x(r, t) = r, \quad y(r, t) = t, \quad z(r, t) = \sin k\pi r, \quad (r, t) \in [0, 1] \times [0, 1],$$

and another one (type 2) by

$$x(r, t) = \sin k\pi r, \quad y(r, t) = r, \quad z(r, t) = t, \quad (r, t) \in [0, 1] \times [0, 1],$$

the former a rotation of the latter by applying the rotation matrix $\begin{pmatrix} 0 & 1 & 0 \\ 0 & 0 & 1 \\ 1 & 0 & 0 \end{pmatrix}$ on the latter, thus of similar shape.

Three plots depicting surfaces (actually their boundaries) of the sine kind for different values of k are shown in Figure 2. (Note that in the plots there, the x -, y -, z - axes are not always to scale relative to one another). In each plot two surfaces of the sine kind appear. The two surfaces in the leftmost plot being of similar shape, clearly the elastic shape

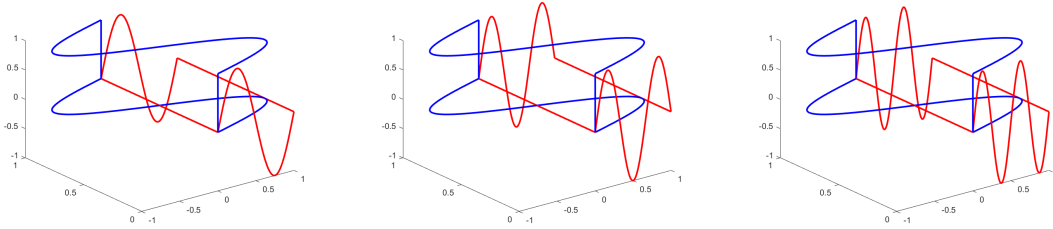


Fig. 2. Three plots of boundaries of surfaces of the sine kind. A partial elastic shape registration of the two surfaces in each plot and the elastic shape distance between them associated with the registration were computed.

distance between them is exactly zero, and the hope was then that the execution of our software package applied on these two surfaces would produce an elastic shape distance between them equal or close to zero. The type 2 surface in each plot (in blue) was considered to be the first surface in the plot. In each plot this surface was obtained by setting k equal to 2 in the definition above of a type 2 surface of the sine kind so that it is the same surface in all three plots. The other surface in each plot (in red) is a type 1 surface of the sine kind and was considered to be the second surface in each plot. From left to right in the three plots, the second surface was obtained by setting k equal to 2, 3, 4, respectively, in the definition above of a type 1 surface of the sine kind. As already mentioned above, in the procedure for optimizing over rotations and reparametrizations using Dynamic Programming as described in Section 7, Procedure DP-surface-min, the second surface is reparametrized while the first one is rotated.

With $\gamma(r, t) = (r^{5/4}, t)$, $(r, t) \in [0, 1] \times [0, 1]$, all surfaces in the plots were then discretized as described above and a partial elastic shape registration of the two surfaces in each plot and the elastic shape distance between them associated with the partial registration were then computed through executions of our software package. We note that for this particular γ , the discretization of the second surface was perturbed only in the r direction which made the software package more likely to succeed as Procedure DP-surface-min always reparametrizes the second surface by applying the Dynamic Programming software exclusively on curves in 3-dimensional space contained in the surfaces in the r direction. The three elastic shape distances, computed in the order of the plots from left to right, were as follows with the first distance, as hoped for, essentially equal to zero: 0.0003 0.3479 0.3192. The times of execution in the same order were 27, 28, 39 seconds, with the **repeat** loop in Procedure DP-surface-min in Section 7 executed 3, 3, 4 times, respectively. The computed optimal rotation matrix for the pair of surfaces in the leftmost plot in Figure 2, was $\begin{pmatrix} 0 & 1 & 0 \\ 0 & 0 & 1 \\ 1 & 0 & 0 \end{pmatrix}$. For the other two pairs of surfaces the computed optimal rotation matrices were both almost equal to $\begin{pmatrix} 0 & 1 & 0 \\ 0 & 0 & 1 \\ 1 & 0 & 0 \end{pmatrix}$ as well, their entries slightly different. It should be pointed out that because of the simplicity of surfaces of the sine kind and the

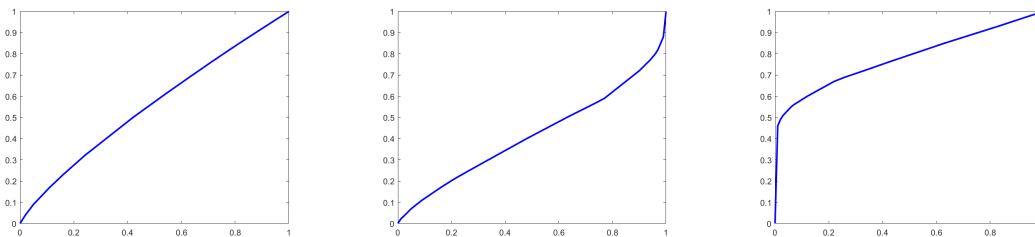


Fig. 3. Graphs of optimal diffeomorphisms from execution of Dynamic Programming software on the three pairs of surfaces with $\gamma(r,t) = (r^{5/4}, t)$, $(r,t) \in [0,1] \times [0,1]$. One per pair, as for each pair the same two curves in 3–d space were used as input to the software each time it was executed. Thus the same diffeomorphism was computed each time for each pair of surfaces.

fact that for the given γ the discretization of the second surface was perturbed only in the r direction, whenever the Dynamic Programming software was executed for a given pair of surfaces, the same two curves in 3–dimensional space contained in the surfaces in the r direction were always used as input to the software. Therefore for the given pair, the same solution was obtained each time (101 times) the Dynamic Programming software was executed, in particular the same optimal orientation-preserving diffeomorphism from $[0,1]$ onto $[0,1]$ was computed each time together with the same elastic shape distance between the two curves in 3–dimensional space used as input to the software. Graphs of the optimal diffeomorphisms for each pair of surfaces in the order of the plots from left to right in Figure 2, are shown in Figure 3. In addition, Figure 4 shows results of the partial elastic shape registration of the pair of surfaces in the rightmost plot in Figure 2. The pair of surfaces is shown in the leftmost plot of the figure before any computations took place. In the middle plot we see the first surface after it was rotated with the corresponding computed optimal rotation matrix mentioned above. In the rightmost plot we see the second surface after it was reparametrized with the homeomorphism on the unit square corresponding to the partial elastic shape registration of the pair of surfaces, a homeomorphism computed based on the optimal diffeomorphism obtained each time (101 times) the Dynamic Programming software was executed for the pair of surfaces, and that because of the simplicity of the surfaces involved and the fact that for the given γ the discretization of the second surface was perturbed only in the r direction, was always the same diffeomorphism, the diffeomorphism whose graph appears in the rightmost plot in Figure 3.

Finally, we note that with $\gamma(r,t) = (r^{5/4}, t^{5/4})$, $(r,t) \in [0,1] \times [0,1]$, the software package was applied on the pair of surfaces in the leftmost plot in Figure 2. The computed elastic shape distance between the two surfaces was 0.0126, the time of execution was 28 seconds, with the **repeat** loop in Procedure DP-surface-min in Section 7 executed 3 times, and the computed optimal rotation matrix for the pair of surfaces was $\begin{pmatrix} 0 & 1 & 0 \\ 0 & 0 & 1 \\ 1 & 0 & 0 \end{pmatrix}$. These results were not far from those obtained with the previous γ , however for the current γ the discretization of the second surface was perturbed in both the r and t directions. As Procedure

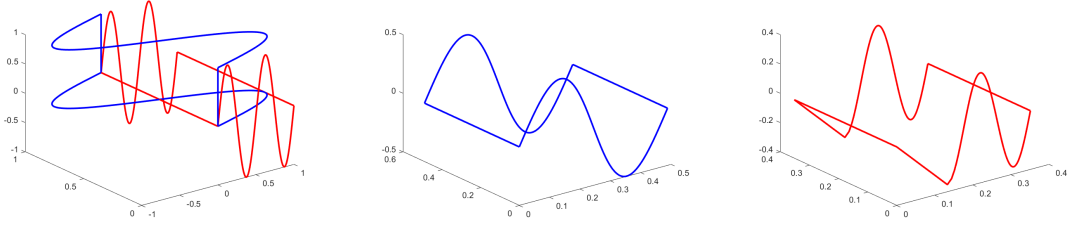


Fig. 4. With $\gamma(r,t) = (r^{5/4}, t)$, $(r,t) \in [0,1] \times [0,1]$, views of boundaries of pair of surfaces in the rightmost plot in Figure 2 before computation of partial elastic shape registration (leftmost plot here), of boundary of optimally rotated first surface (middle plot), and of boundary of optimally reparametrized second surface (rightmost plot) after computations.

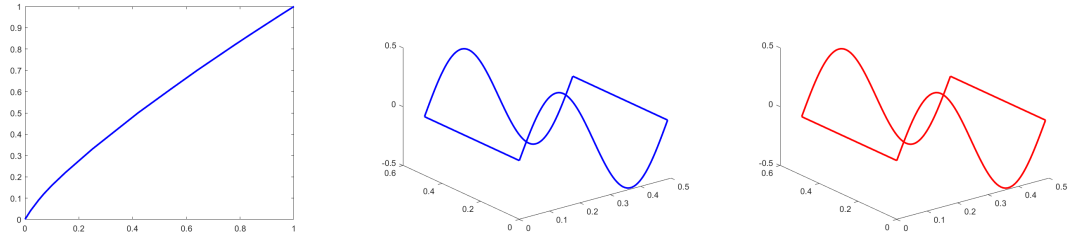


Fig. 5. For $\gamma(r,t) = (r^{5/4}, t^{5/4})$, $(r,t) \in [0,1] \times [0,1]$, views of graph of optimal diffeomorphism computed the 51st time the Dynamic Programming software was executed (leftmost plot), of boundary of optimally rotated first surface (middle plot), and of optimally reparametrized second surface (rightmost plot) after computation of partial elastic shape registration.

DP-surface-min is not equipped to handle perturbations in the t direction, perhaps this was the reason why the computed elastic shape distance between the two surfaces was not exactly zero as in particular the optimal orientation-preserving diffeomorphisms from $[0,1]$ onto $[0,1]$ computed with the Dynamic Programming software differed slightly from one another, while the computed elastic shape distances between the curves in 3-dimensional space used as input to the software differed from one another as well and were not exactly close to zero. The graph of the optimal diffeomorphism computed the 51st time the Dynamic Programming software was executed is shown in Figure 5 together with results of the partial elastic shape registration of the pair of surfaces. It should be noted here that perhaps as long as the second surfaces we have chosen for testing the software are perturbed in the same manner in the r direction, it is likely the graphs of the optimal diffeomorphisms computed with the Dynamic Programming software will tend to resemble one another regardless of the surfaces involved.

The next results that follow were obtained from applications of our software package on discretizations of surfaces in 3-dimensional space of the helicoid kind. Given k , a positive integer, one type of surface to which we refer as a surface of the helicoid kind (type 1) is

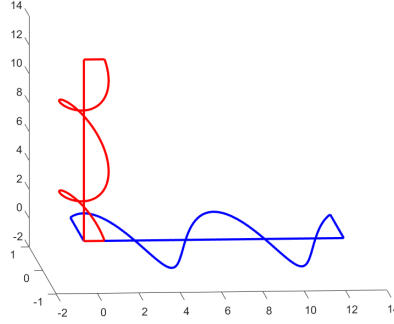


Fig. 6. Boundaries of two surfaces of similar shape of the helicoid kind for $k = 4$, type 1 in red, type 2 in blue.

defined by

$$x(r,t) = r \cos k\pi t, \quad y(r,t) = r \sin k\pi t, \quad z(r,t) = k\pi t, \quad (r,t) \in [0,1] \times [0,1],$$

and another one (type 2) by

$$x(r,t) = k\pi t, \quad y(r,t) = r \cos k\pi t, \quad z(r,t) = r \sin k\pi t, \quad (r,t) \in [0,1] \times [0,1],$$

the former a rotation of the latter by applying the rotation matrix $\begin{pmatrix} 0 & 1 & 0 \\ 0 & 0 & 1 \\ 1 & 0 & 0 \end{pmatrix}$ on the latter, thus of similar shape.

A plot depicting two surfaces (actually their boundaries) of similar shape of the helicoid kind for $k = 4$ is shown in Figure 6. (Note that in the plot there, the x -, y -, z - axes are not always to scale relative to one another). The two surfaces being of similar shape, clearly the elastic shape distance between them is exactly zero, and the hope was once again that the execution of our software package applied on these two surfaces would produce an elastic shape distance between them equal or close to zero. The type 2 surface of the helicoid kind in the plot (in blue) was considered to be the first surface in the plot. The other surface in the plot (in red) is a type 1 surface of the helicoid kind and was considered to be the second surface in the plot.

With $\gamma(r,t) = (r^{5/4}, t)$, $(r,t) \in [0,1] \times [0,1]$, the two surfaces in the plot were then discretized as described above and a partial elastic shape registration of the two surfaces and the elastic shape distance between them associated with the partial registration were then computed through the execution of our software package. Again we note that for this particular γ , the discretization of the second surface was perturbed only in the r direction which as pointed out above made the software package more likely to succeed. The computed distance was 0.0002, which, as hoped for, was close enough to zero. The time of execution was 15 seconds with the **repeat** loop in Procedure DP-surface-min in Section 7 executed 2 times. The computed optimal rotation matrix for the pair of surfaces was $\begin{pmatrix} 0 & 1 & 0 \\ 0 & 0 & 1 \\ 1 & 0 & 0 \end{pmatrix}$. As was

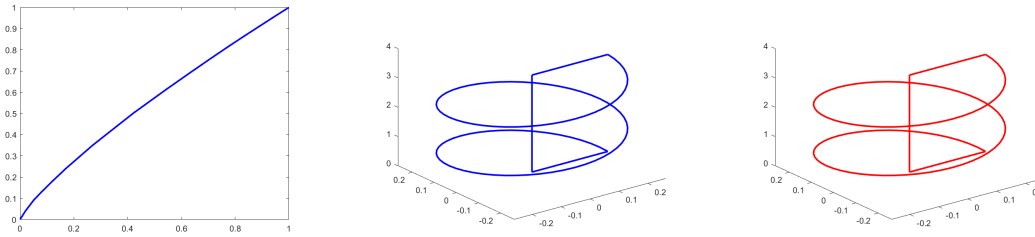


Fig. 7. For $\gamma(r,t) = (r^{5/4}, t)$, $(r,t) \in [0, 1] \times [0, 1]$, views of graph of optimal diffeomorphism computed each time the Dynamic Programming software was executed on pair of surfaces (leftmost plot), of boundary of optimally rotated first surface (middle plot), and of optimally reparametrized second surface (rightmost plot) after computation of partial elastic shape registration.

the case for surfaces of the sine kind, once again essentially the same solution was obtained each time the Dynamic Programming software was executed as essentially the same two curves in 3–dimensional space contained in the surfaces in the r direction were used each time as input to the software (the same two curves in the sense that given a pair of curves used as input, the two curves had the same shape and that shape was the same shape of each curve in any other pair used as input to the Dynamic Programming software). In particular, essentially the same optimal orientation-preserving diffeomorphism from $[0, 1]$ onto $[0, 1]$ was computed each time together with the same elastic shape distance close to zero between the two curves in 3–dimensional space used as input to the software. The graph of this optimal diffeomorphism is shown in Figure 7 together with results of the partial elastic shape registration of the pair of surfaces.

Finally, we note that with $\gamma(r,t) = (r^{5/4}, t^{5/4})$, $(r,t) \in [0, 1] \times [0, 1]$, the software package was applied again on the pair of surfaces. The computed elastic shape distance between the two surfaces was 0.0796, the time of execution was 19 seconds, with the **repeat** loop in Procedure DP-surface-min in Section 7 executed 2 times, and the computed optimal rotation matrix for the pair of surfaces was approximately $\begin{pmatrix} .028 & .762 & .647 \\ -.029 & -.646 & .763 \\ .999 & -.040 & .004 \end{pmatrix}$. These results were not as good as those obtained with the previous γ but still acceptable considering that for the current γ the discretization of the second surface was perturbed in both the r and t directions. As mentioned above Procedure DP-surface-min is not equipped to handle perturbations in the t direction, so perhaps this was the reason why the computed elastic shape distance between the two surfaces was not exactly zero as in particular the optimal orientation-preserving diffeomorphisms from $[0, 1]$ onto $[0, 1]$ computed with the Dynamic Programming software differed slightly from one another, while the computed elastic shape distances between the curves in 3–dimensional space used as input to the software differed from one another as well and were not exactly close to zero. This inability to handle perturbations in the t direction may have also affected the computation of the optimal rotation matrix. The graph of the optimal diffeomorphism computed the 51st time the Dynamic Pro-

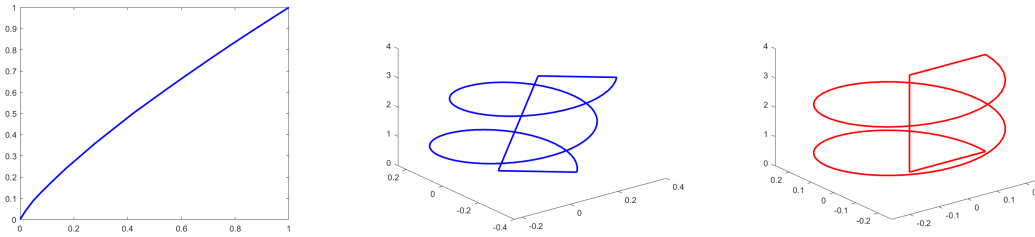


Fig. 8. For $\gamma(r,t) = (r^{5/4}, t^{5/4})$, $(r,t) \in [0,1] \times [0,1]$, views of graph of optimal diffeomorphism computed the 51st time the Dynamic Programming software was executed (leftmost plot), of boundary of optimally rotated first surface (middle plot), and of optimally reparametrized second surface (rightmost plot) after computation of partial elastic shape registration.

gramming software was executed is shown in Figure 8 together with results of the partial elastic shape registration of the pair of surfaces. Once again we note that perhaps as long as the second surfaces we have chosen for testing the software are perturbed in the same manner in the r direction, it is likely the graphs of the optimal diffeomorphisms computed with the Dynamic Programming software will tend to resemble one another regardless of the surfaces involved.

The final results that follow were obtained from applications of our software package on discretizations of surfaces in 3–dimensional space that are actually graphs of 3–dimensional functions based on the product of the cosine and sine functions. One surface of this kind to which we refer as a surface of the cosine-sine kind (type 1) is defined by

$$x(r,t) = r, \quad y(r,t) = t, \quad z(r,t) = (\cos 0.5\pi r)(\sin 0.5\pi t), \quad (r,t) \in [0,1] \times [0,1],$$

and another one (type 2) by

$$x(r,t) = (\cos 0.5\pi r)(\sin 0.5\pi t), \quad y(r,t) = r, \quad z(r,t) = t, \quad (r,t) \in [0,1] \times [0,1],$$

the former a rotation of the latter by applying the rotation matrix $\begin{pmatrix} 0 & 1 & 0 \\ 0 & 0 & 1 \\ 1 & 0 & 0 \end{pmatrix}$ on the latter, thus of similar shape.

A plot depicting two surfaces (actually their boundaries) of similar shape of the cosine-sine kind is shown in Figure 9. (Note that in the plot there, the x –, y –, z – axes are not always to scale relative to one another). The two surfaces being of similar shape, clearly the elastic shape distance between them is exactly zero, and the hope was once again that the execution of our software package applied on these two surfaces would produce an elastic shape distance between them equal or close to zero. The type 2 surface of the cosine-sine kind in the plot (in blue) was considered to be the first surface in the plot. The other surface in the plot (in red) is a type 1 surface of the cosine-sine kind and was considered to be the second surface in the plot.

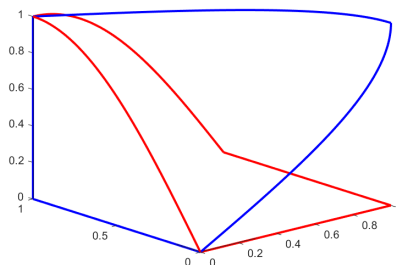


Fig. 9. Boundaries of two surfaces of similar shape of the cosine-sine kind, type 1 in red, type 2 in blue.

With $\gamma(r,t) = (r^{5/4}, t)$, $(r,t) \in [0,1] \times [0,1]$, the two surfaces in the plot were then discretized as described above and a partial elastic shape registration of the two surfaces and the elastic shape distance between them associated with the partial registration were then computed through the execution of our software package. Again we note that for this particular γ , the discretization of the second surface was perturbed only in the r direction which as pointed out above made the software package more likely to succeed. The computed distance was 0.0002, which, as hoped for, was close enough to zero. The time of execution was 22 seconds with the **repeat** loop in Procedure DP-surface-min in Section 7 executed 3 times. The computed optimal rotation matrix for the pair of surfaces was essentially $\begin{pmatrix} 0 & 1 & 0 \\ 0 & 0 & 1 \\ 1 & 0 & 0 \end{pmatrix}$. It should be noted here that the type 1 surface of the cosine-sine kind satisfies that given t_1, t_2 , $0 \leq t_1 < t_2 \leq 1$, then the two 3-dimensional curves in the surface obtained by fixing t to t_1 and t to t_2 , have different shapes. In spite of this, the optimal orientation-preserving diffeomorphisms from $[0,1]$ onto $[0,1]$ computed with the Dynamic Programming software for the given γ , although differing from one another, differed only very slightly, while the computed elastic shape distances between the curves in 3-dimensional space used as input to the software were all very close to zero. The graph of the optimal diffeomorphism computed the 51st time the Dynamic Programming software was executed is shown in Figure 10 together with results of the partial elastic shape registration of the pair of surfaces.

Finally, we note that with $\gamma(r,t) = (r^{5/4}, t^{5/4})$, $(r,t) \in [0,1] \times [0,1]$, the software package was applied again on the pair of surfaces. The computed elastic shape distance between the two surfaces was 0.0143, the time of execution was 23 seconds, with the **repeat** loop in Procedure DP-surface-min in Section 7 executed 3 times, and the computed optimal rotation matrix for the pair of surfaces was approximately $\begin{pmatrix} -.043 & .999 & .026 \\ -.035 & -.028 & .999 \\ .998 & .042 & .036 \end{pmatrix}$. These results although not as good as those obtained with the previous γ were still acceptable considering once again that for the current γ the discretization of the second surface was perturbed in both the r and t directions. Again as mentioned above Procedure DP-surface-min is not

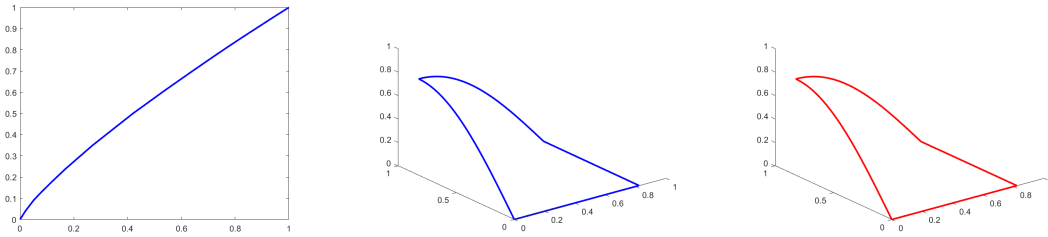


Fig. 10. For $\gamma(r,t) = (r^{5/4}, t)$, $(r,t) \in [0,1] \times [0,1]$, views of graph of optimal diffeomorphism computed the 51st time the Dynamic Programming software was executed on pair of surfaces (leftmost plot), of boundary of optimally rotated first surface (middle plot), and of optimally reparametrized second surface (rightmost plot) after computation of partial registration.

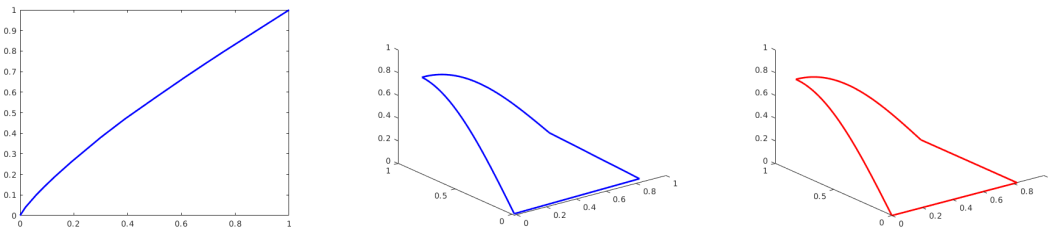


Fig. 11. For $\gamma(r,t) = (r^{5/4}, t^{5/4})$, $(r,t) \in [0,1] \times [0,1]$, views of graph of optimal diffeomorphism computed the 51st time the Dynamic Programming software was executed (leftmost plot), of boundary of optimally rotated first surface (middle plot), and of optimally reparametrized second surface (rightmost plot) after computation of partial elastic shape registration.

equipped to handle perturbations in the t direction, so perhaps this was the reason why the computed elastic shape distance between the two surfaces was not exactly zero as in particular the optimal orientation-preserving diffeomorphisms from $[0,1]$ onto $[0,1]$ computed with the Dynamic Programming software differed slightly from one another, while the computed elastic shape distances between the curves in 3-dimensional space used as input to the software differed from one another as well and were not exactly close to zero. The graph of the optimal diffeomorphism computed the 51st time the Dynamic Programming software was executed is shown in Figure 11 together with results of the partial elastic shape registration of the pair of surfaces. Once again we note that perhaps as long as the second surfaces we have chosen for testing the software are perturbed in the same manner in the r direction, it is likely the graphs of the optimal diffeomorphisms computed with the Dynamic Programming software will tend to resemble one another regardless of the surfaces involved.

9. Summary

In this paper we have presented an algorithm for computing, using Dynamic Programming, a partial elastic shape registration of two simple surfaces in 3-dimensional space together with the elastic shape distance between them associated with the partial registration. The algorithm we have presented minimizes a distance function of the surfaces in terms of rotations of one of the surfaces and a special subset of the set of reparametrizations of the other surface, the optimization over reparametrizations based on the computation, using Dynamic Programming, of the elastic shape registration of pairs of simple curves in 3-dimensional space contained in the surfaces. This algorithm does not necessarily compute an optimal elastic shape registration of the surfaces together with the exact elastic shape distance between them, but perhaps a registration and a distance closer to optimal than those obtained with an algorithm based on a gradient approach over the entire set of reparametrizations of one of the surfaces. In fact we propose that when computing the elastic shape registration of two simple surfaces and the elastic shape distance between them with an algorithm based on a gradient approach for optimizing over the entire set of reparametrizations of one of the surfaces, to use as the input initial solution the rotation and the reparametrization computed with our proposed algorithm. Finally, we note, promising results from computations with the implementation of our methods applied on three simple kinds of 3-dimensional surfaces, have been presented in this paper. A link to the software package, etc., has been given as well.

References

- [1] Bernal, J., Dogan, G., Hagwood, C. R.: Fast Dynamic Programming for Elastic Registration of Curves. Proceedings of DIFF-CVML workshop, CVPR 2016, Las Vegas, Nevada. (2016)
- [2] Bernal, J.: Shape Analysis, Lebesgue Integration and Absolute Continuity Connections. NISTIR 8217 (2018).
- [3] Bernal, J., Lawrence, J.: Characterization and Computation of Matrices of Maximal Trace Over Rotations. Journal of Geometry and Symmetry in Physics. 53 (2019).
- [4] Bernal, J., Lawrence, J., Dogan, G., Hagwood, C. R.: On Computing Elastic Shape Distances between Curves in d-dimensional Space. NIST Technical Note 2164 (2021)
- [5] Dogan, G., Bernal, J., Hagwood, C. R.: FFT-based alignment of 2d closed curves with application to elastic shape analysis. Proceedings of the 1st DIFF-CV Workshop, British Machine Vision Conference, Swansea, Wales, UK. September 2015.
- [6] Jermyn, I. H., Kurtek, S., Klassen, E., and Srivastava, A.: Elastic shape matching of parameterized surfaces using square root normal fields. Proceedings of the 12th European Conference on Computer Vision (ECCV'12), Volume V, pp. 804–817. Springer, Berlin (2012)
- [7] Joshi, S. H., Klassen, E., Srivastava, A., and Jermyn, I. H.: A novel representation for riemannian analysis of elastic curves in R^n . Proceedings of the IEEE Conference on Computer Vision and Pattern Recognition (CVPR), Minneapolis, MN. June 2007.
- [8] Kabsch, W.: A solution for the best rotation to relate two sets of vectors. Acta Crystallographica Section A: Crystal Physics. 32(5): 922-923 (1976).
- [9] Kabsch, W.: A discussion of the solution for the best rotation to relate two sets of vectors. Acta Crystallographica Section A: Crystal Physics. 34(5): 827-828 (1978).
- [10] Kurtek, S., Klassen, E., Ding, Z., Srivastava, A.: A novel riemannian framework for shape analysis of 3D objects. Proceedings of the IEEE Conference on Computer Vision and Pattern Recognition (CVPR), San Francisco, CA. June 2010.
- [11] Lawrence, J., Bernal, J., Witzgall, C.: A Purely Algebraic Justification of the Kabsch-Umeyama Algorithm. Journal of Research of the National Institute of Standards and Technology. 124 (2019).
- [12] Lay D., Lay S. and McDonald J.: *Linear Algebra and its Applications*, 5th edition, Pearson Education, Boston 2016.
- [13] Salvador, S., Chan, P.: FastDTW: Toward Accurate Dynamic Time Warping in Linear Time and Space. 3rd Wkshp. on Mining Temporal and Sequential Data, ACM KDD '04. (2004)
- [14] Srivastava, A., Klassen, E. P.: Functional and Shape Data Analysis. New York: Springer. (2016)
- [15] Srivastava, A., Klassen, E. P., Joshi, S. H., Jermyn, I. H.: Shape Analysis of Elastic Curves in Euclidean Spaces. IEEE Trans. Pattern Analysis and Machine Intelligence. 33(7): 1415-1428 (2011).
- [16] Umeyama, S.: Least-Squares Estimation of Transformation Parameters Between Two

Point Patterns. IEEE Trans. Pattern Analysis and Machine Intelligence. 13(4): 376-380 (1991).